PCCP

Accepted Manuscript

ROYAL SOCIETY OF CHEMISTRY

www.rsc.org/pccp

Introduction to the chemistry of graphene

Xiluan Wang[a,b] and Gaoquan Shi*[a]

[a] *Department of Chemistry, Tsinghua University, Beijing 100084, People's Republic of China*

[b] *Beijing Key Laboratory of Lignocellulosic Chemistry, Beijing Forestry University, Beijing 100083, People's Republic of China*

Pristine graphene and chemically modified graphenes (CMGs, e.g., graphene oxide, reduced graphene oxide and their derivatives) can occur a variety of chemical reactions. These reactions have been applied to modulate the structures and properties of graphene materials, and to extend their functions and practical applications. This perspective outlines the chemistry of graphene, including functionalization, doping, photochemistry, catalytic chemistry, and supramolecular chemistry. The mechanisms of graphene related reactions will be introduced, and the challenges of controlling the chemical reactions of graphene will be discussed.

Introduction

Graphene has a unique atom–thick two–dimensional structure, and excellent electrical, optical, chemical, thermal, and mechanical properties.[1,2] It is an attractive material for a variety of applications, including electronics,[3,4] energy related systems,[5,6] sensors,[7,8] actuators,[9,10] and composites,[11,12] etc. To satisfy the requirements in practical applications, graphene frequently has to be chemically modified.[13,14] First, pristine graphene is insoluble and intractable, and decomposes before melting.[15] Thus, the conventional material processing techniques cannot be applied to shape it into desired structures. Second, graphene layers can only be physically stabilized on solid supports.[16,17] Free–standing graphene layers tend to form wrinkles or to stack together through π–π and hydrophobic interactions.[18] Third, graphene is a zero bandgap material.[19] Opening the bandgap of graphene is a prerequisite for its applications in electronics or optoelectronics.[2] Fourth, pristine graphene usually has poor catalytic performance,[20] and weak interactions with other small molecules or polymers,[21] limiting their applications in catalysis, sensors, and composites. To address these issues, several chemical methods have been developed to modify the surfaces and electronic structures of graphene sheets.

Chemical functionalization is an effective approach to modify the structure and properties of graphene.[14,22] By selectively attaching functionalities on their surfaces, graphene sheets can be homogeneously dispersed in aqueous and/or organic media.[23,24] On the other hand, the covalent attachment of chemical groups leads to the transition of carbon hybridization from sp^2 to sp^3, possibly to open a tunable bandgap

in graphene.[24,25] Furthermore, chemical functionalization can modulate the optical, chemical, and mechanical properties of graphene materials.[15,26]

Heteroatom doping can effectively tune the electronic structure and intrinsic properties of graphene.[27] This technique can also open a bandgap near the Fermi level, changing graphene from a "metallic" material to a "semiconductor".[28] By covalently bonding the electron donating or withdrawing complexes to graphene, a p–type or n–type material would be produced. These materials have unique electrical, magnetic and optical properties, making them have promising applications in supercapacitors, catalysis, batteries, and field emission, etc. [29–31]

On the other hand, the chemical reactivity of graphene basal plane is weak because of its giant π-conjugation system, little structure curvature and the absence of dangling bonds.[15,32] Thus, most chemical reactions can only occur at the edges or the defective sites of graphene sheets.[33,34] Chemical reactions on the basal plane of graphene have a large energy barrier, requiring highly reactive species to initiate the reaction. Photochemical process can generate reactive free radicals to react with graphene basal planes.[35]

Adsorption is another efficient strategy to modulate the surface structure and properties of graphene.[21] The graphitic carbon atoms have an intriguing potential to chemisorb the reactants and form surface intermediates.[36] CMGs with functional groups exhibit high adsorbing reactivity under mild conditions.[37–39] Pristine graphene can also make the use of its delocalized π–electron system to form chemisorbed products.[40,41] The chemisorbing approaches have been widely to develop new

graphene based catalysts.

CMG sheets can be regarded as 2D conjugated macromolecules with huge molar masses, having supramolecular chemistry.[42] A graphene oxide (GO) sheet behaves like an amphiphilic macromolecule with hydrophilic edges and a hydrophobic basal plane.[43] Chemically functionalized reduced graphene oxide (rGO) also exhibits molecular behaviour.[44] Thus, they can be assembled into macroscopic materials with controlled compositions and microstructures via hydrogen bonding, hydrophobic, π–π stacking and/or electrostatic interaction between graphene sheets.

Several excellent reviews have partly summarized the chemistry of graphene.[13,32,45] However, an article that comprehensively outlines the chemistry of graphene has not yet been published. Here, we try to provide an introduction to the chemistry of graphene from different aspects including functionalization, doping, catalytic chemistry, photochemistry and supramolecular chemistry. To limit the length of this article, we selected typical reactions as examples; many excellent papers are possibly not included. The chemical reactions discussed here are also involved in the preparation of graphene materials including composites for the applications in sensors, catalysis, environmental protection and energy related systems, etc. Nevertheless, the details about the synthesis of graphene composites, and the applications of graphene materials will not be summarized here, because they are the topics of many existing reviews. This perspective focuses on the inherent chemistry related to pristine graphene and its derivatives.

1. Functionalization

The synthesis and applications of functionalized graphene materials have already been summarized in several reviews.[45–47] However, few of them systematically discussed the chemistry related to the functionalization of graphene. In this section, we focus on the reaction mechanisms of graphene functionalization, and the structural and property changes of graphene upon functionalization. Fig. 1 schematically illustrates the chemical functionalization of graphene through covalent or noncovalent approach.[48] The edge sites of a graphene sheet with dangling bonds are more reactive than its basal plane. The dangling bonds can be used to covalently bonding with various chemical moieties (Fig. 1a). These chemical moieties can increase the

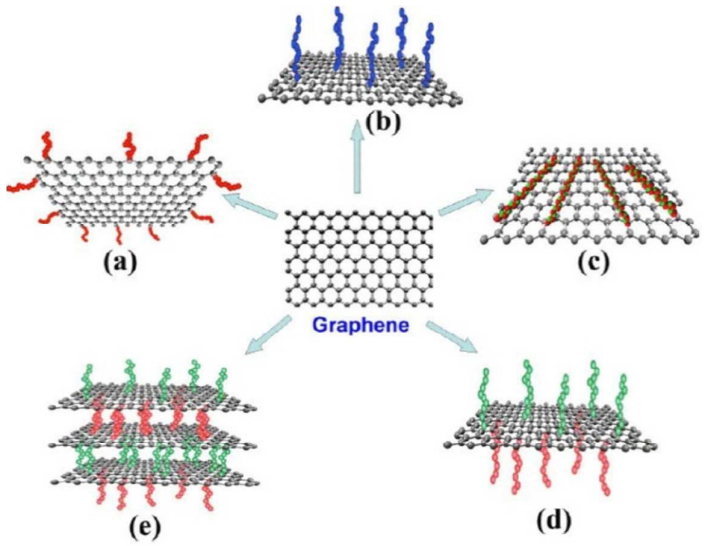

Fig. 1 Chemical functionalization of graphene: (a) edge–functionalization, (b) basal–plane–functionalization, (c) noncovalent adsorption on the basal plane, (d) asymmetrical functionalization of the basal plane, and (e) self–assembly of functionalized graphene sheets. Reproduced from reference 48 with permission.

solubility and processability of graphene, or provide reactive groups for further modification. Covalently functionalization of graphene basal plane (Fig. 1b) causes the distortion of π–π conjugation system. In contrast, the noncovalent functionalization keeps the atomic and electronic structures of graphene (Fig. 1c)). The asymmetric functionalization on the two surfaces of a graphene sheet (Fig. 1d) can provide graphene with specific supramolecular behavior (Fig. 1e).

1.1 Covalent functionalization of graphene basal plane

The basal plane of graphene composes of sp^2 carbons, which is chemically unsaturated. Intrinsically, it is possible to undergo covalent addition to change the carbon atoms from sp^2 to sp^3 hybridization. In this process, the planar aromatic carbons transform to a tetrahedral geometry with longer bonds. This functionalization creates a geometric distortion, thus encounters high energy barriers. The covalent functionalization requires high energy reactants, such as hydrogen atoms, fluorine atoms, strong acids, and radicals.

1.1.1 Hydrogenation

Hydrogenation is the most thoroughly studied covalent addition reaction on the basal plane of graphene.[49–52] The hydrogenated graphene has been prepared by using atomic hydrogen beams, in which molecular hydrogen is cracked on a hot filament, or via exposure to hydrogen–based plasmas.[53,54] This reaction changes the hybridization of carbon atoms from sp^2 to sp^3, resulting in elongating C–C bonds in the

hydrogenated graphene. Hydrogen atoms tend to react with both sides of the basal plane of pristine graphene. If only one side is hydrogenated, the graphene sheet would roll into a tube because of the unbalanced external stress.[55] The fully hydrogenated graphene is called "graphane", and every carbon atom of graphane is covalently bonded to a hydrogen atom.[56] As a consequence, the graphene layer was buckled. Fig. 2 shows the schematic structures of three stable graphane isomers with chair, stirrup, and boat configurations, together with two other isomers.[57] Computational studies indicate that the chair configuration is the most stable one. In this configuration, the H atoms are alternately adsorbed above and below the graphene sheet (Fig. 2a). The stirrup configuration, also called zigzag or washboard configuration, is more stable than the boat configuration. The stirrup isomer consists of alternating zigzag chains with H atoms pointing up and down (Fig. 2).

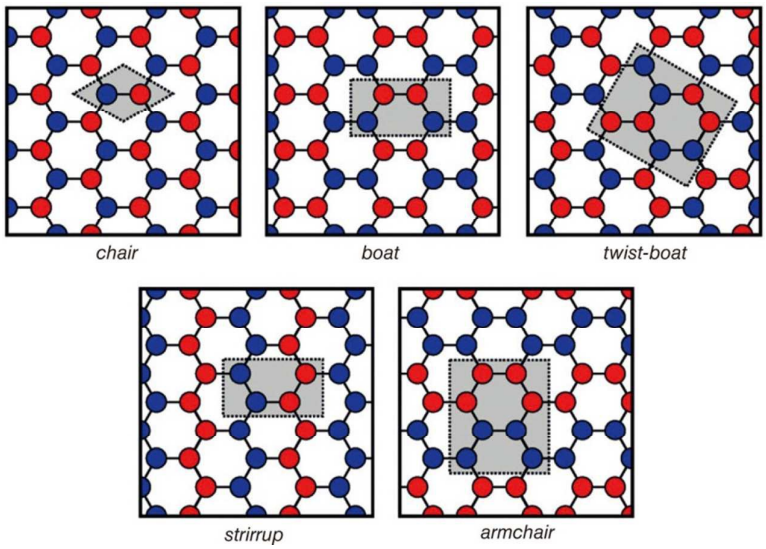

Fig. 2 Five isomers of graphane in which every carbon atom is equivalent. Blue and red colors indicate hydrogen adsorption above and below the graphene layer. Reproduced from reference 57 with permission.

The addition of hydrogen atoms has been predicted to radically change the electronic structure and properties of graphene. Fully hydrogenated graphene is expected to have a wide bandgap. Different calculation methods provided different values. Typically, an adequate approximation of Green function and screened Coulomb–interaction W (GW approximation) has given a bandgap of 5.4 eV.[58] Lowering the hydrogenation degree of graphene narrows the bandgap. Hydrogenated graphene has optical properties different from that of pristine graphene. For example, the optical adsorption spectrum of graphane shows adsorption onset in ultraviolet region, making it to be completely transparent in visible region.[59] Partially hydrogenated graphane shows magnetic properties. Furthermore, the change in hybridization from sp^2 to sp^3 enhances the spin–orbit by two orders of magnitude, making it to be comparable to that of diamond.[60] Hydrogenation increases the elasticity of graphene sheet, because the strong aromatic bond network is replaced with single σ bonds. Perfect graphane behaves elastically under strains up to at least 30%, leading to a higher surface roughness than that of graphene.[61]

1.1.2 Fluorination

Fluorination of graphene is similar to hydrogenation. A fluorine atom connects to carbon with a single bond; however, this bond has a reversed dipole and a stronger binding strength compared with those of the C–H bonds in graphane.[59] The binding energy of C–F bond is lower than that of C–H bond; thus, it would be easier to produce a saturated fluorographene compared to form a graphane. As only one side of

graphene was exposed to fluorine, the fluorination was expected to have a maximum coverage of 25% (C_4F).[62] For double–side fluorinated graphene, the most stable structure is an alternating conformation analogous to the chair conformation of graphane.[63] Fluorination of graphene can be performed mainly by two methods: (1) treating graphene with an appropriate fluorinating regent (e.g., XeF_2);[62,64] (2) chemical or mechanical exfoliation of graphite fluoride.[65]

Theoretical calculation predicted that fluorographene is electrically insulating with a minimal direct bandgap of 3.1 eV.[59] When electron–electron interactions are taken into account within the GW approximation, the calculated bandgap further increased to 7.4 eV.[66,67] Similar to graphane, fluorinated graphene possesses unique optical property. Compared with graphene, partially fluorinated graphene shows higher transparency. Fluorographene appears to be transparent at visible frequencies and only starts to adsorb light in the blue region.[59]

1.1.3 Oxidation

Oxidation is one of the most important chemical reactions of graphene. The addition of oxygen atoms to graphene is a more complex reaction than fluorination or hydrogenation, because an oxygen atom can form two covalent bonds rather than one. Three chemical routes have been developed for the oxidation of graphene. The first is directly oxidize graphene with strong oxidants such as concentrated sulfuric acid, concentrated nitric acid, or potassium permanganate.[68] The second is the oxidation of graphite through Hummers',[69] Brodies',[70] Staudenmaiers'[71] or electrochemical

methods,[72,73] followed by exfoliation. During the oxidation processes, graphite flakes were broken down into smaller fragments. The third oxidation process is lengthwise cutting and unraveling carbon nanotubes (CNTs).[74,75]

GO, an oxidation product of graphene, is one of the most famous graphene derivatives. Typically, it composes of about 45 mass % carbon. Although several structure models have been proposed, GO is a rather polydisperse material; its exact structure is very difficult to be precisely defined. The most widely accepted structure model for GO has been proposed by Lerf and Klinowski (Fig. 3).[76] Accordingly, the functional groups on the basal plane of GO are mainly epoxy and hydroxyl, and the carboxyl groups are mostly located at edge. This structure has been supported by the solid–state nuclear magnetic resonance (NMR) spectra of GO.[77] Theoretical calculations indicate that a GO with a saturated coverage of epoxy groups on its basal plane has a bandgap >3 eV.[78] When the top layer of a bilayer graphene was decorated with epoxy groups, the semimetallic electronic structure of monolayer graphene can be recovered.[79] Because the existence of oxygenated groups, GO can be easily dispersed in aqueous media. GO can also be further functionalized through chemical reactions at its oxygen containing groups.

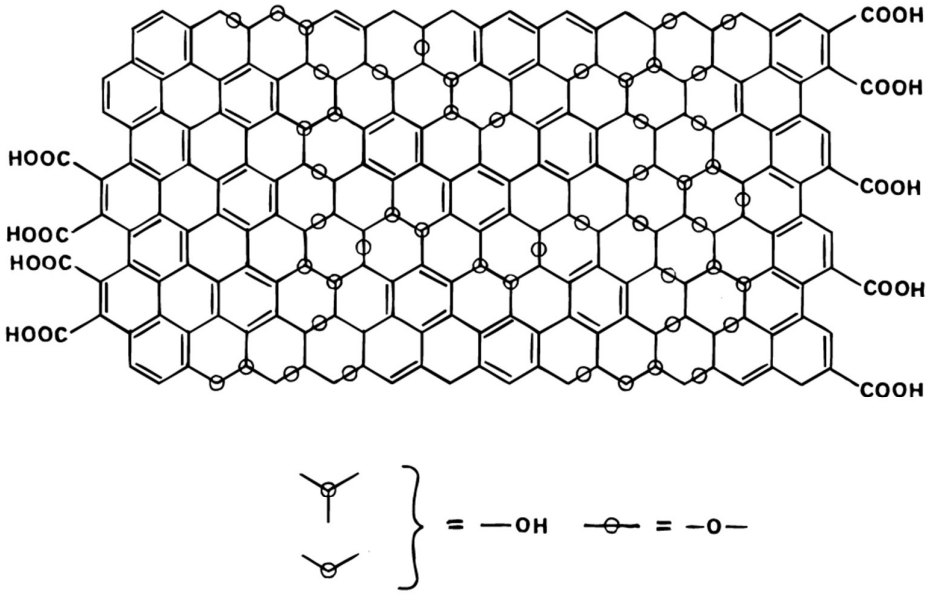

Fig. 3 Lerf–Klinowski structure model of GO. Reproduced from reference 76 with permission.

1.1.4 Free radical addition

Free radical species can frequently overcome the chemical inert nature of pristine graphene. The most widely applied adducts for free radical additions are aryl diazonium salts. Graphene has an electron–rich basal plane because of its π–electrons. When an aryl radical attacks the basal plane of graphene, electrons can transfer from graphene to the radical (Fig. 4).[45,80] The zero bandgap of graphene can be opened by diazonium functionalization. For example, Haddon et al. reported the reaction between epitaxial graphene and (p–nitrophenyl) diazonium tetrafluoroborate, and the resulting functionalized graphene exhibited a bandgap of 0.36 eV.[81] Covalent attachment of the aryl group on the basal plane of graphene converted sp^2 carbon to sp^3. The free radical addition also modified the conjugation length of delocalized

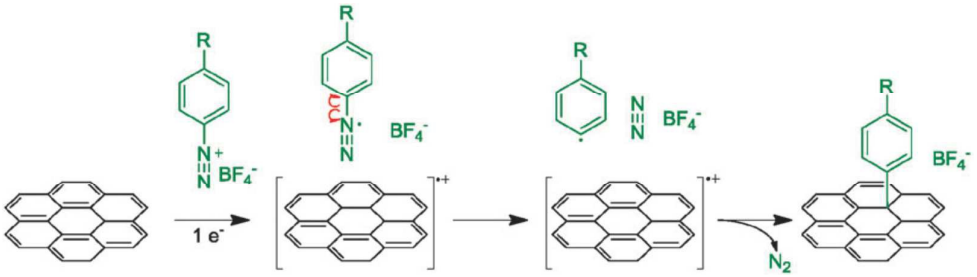

Fig. 4 Mechanism of the free radical addition for derivatives of phenyl onto graphene. Reproduced from reference 45 with permission.

carbon lattice. Both CMG and pristine graphene have been successfully modified by diazonium functionalization at room temperature.[81,82] After functionalization, the solubility of graphene in polar aprotic solvents (e.g. dimethylformamide (DMF), Dimethylacetamide (DMAc) and N–Methyl pyrrolidone (NMP)) was increased. In addition, the nitro groups of diazotized graphene can be reduced to amine groups for further modifying graphene via the reactions of amine groups with hydroxyl, carboxyl or acyl chloride groups of other functional components.

1.1.5 Cycloaddition reaction

Cycloaddition reactions differ from most typical organic reactions, because these reactions do not produce anions or cations as intermediates. Instead, the electrons move in a circular manner that involves simultaneous bond cleavage and bond formation. According to the atom number of addition ring, the cycloaddition functionalization of graphene include four types: [2+1] cycloaddition forming three–membered ring, [2+2] cycloaddition forming four–membered ring, [3+2]

cycloaddition forming five–membered ring and [4+2] cycloaddition forming six–membered ring.[45]

The [2+1] cycloaddition is one of the earliest adopted methods to functionalize the sp^2 carbon network of graphene. Carbene and nitrene are two typical intermediates for this purpose. For instance, dichlorocarbene has been successfully coupled to the sp^2 carbon network of graphene (Fig. 5a) because of its high reactivity.[45,83] In this case, the singlet carbene (an electrophile) reacts spontaneously with the sp^2 carbon atoms; the empty p orbital of carbene (LUMO) interacts with the π bond (HOMO) of the C=C, and the electron pair of carbene (HOMO) interacts with the π* antibonding orbital (LUMO) of the C=C.[84] Thus, the dichlorocarbene addition perturbs the π conjugation of graphene, changing the electronic property of graphene from metallic to semiconducting. Furthermore, the introduction of polar chloride atoms increases the the solubility of graphene in organic solvents. The cyclopropane adduct can tune the energy gap of graphene. Similar to carbene, nitrene intermediates lead to the formation of aziridine adducts onto graphene (Fig. 5b).[85]

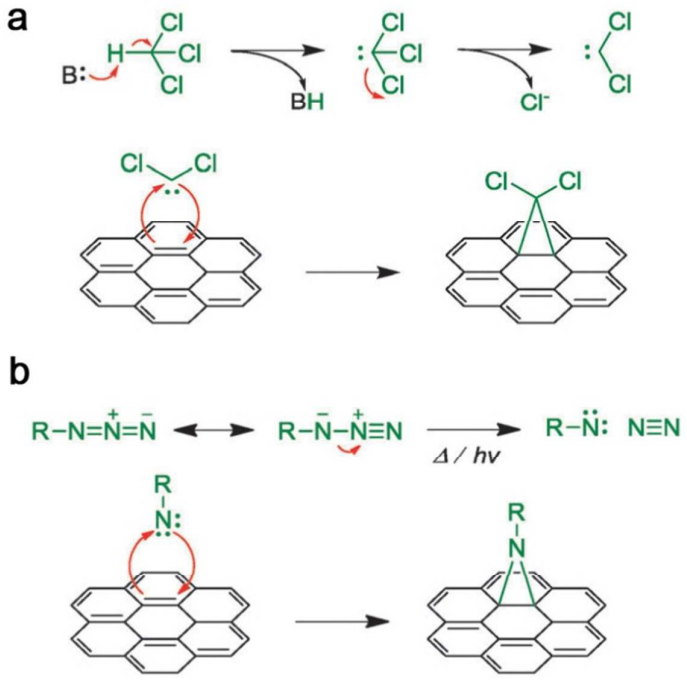

Fig. 5 (a) Mechanism of the formation of dichlorocarbene with chloroform and base (top), and cyclopropanation of graphene with dichlorocarbene (bottom). (b) Mechanism of the formation of nitrene via the decomposition of azide (top) and cycloaddition of nitrene onto graphene (bottom). Reproduced from reference 45 with permission.

In the cases of using aryne or benzyne as the reactive species, four–electron cycloadditions occurred on graphene sp^2 carbon network via an elimination–addition mechanism. Taking fluoride–induced benzyne as an example, the electrophilic benzyne attacks the C=C bond on graphene basal plane, resulting in a [2+2] cycloaddition (Fig. 6a).[45] A five–membered ring can be achieved via a six–electron cycloaddition between a 1,3–dipole and sp^2 carbon atoms on graphene (Fig. 6b).

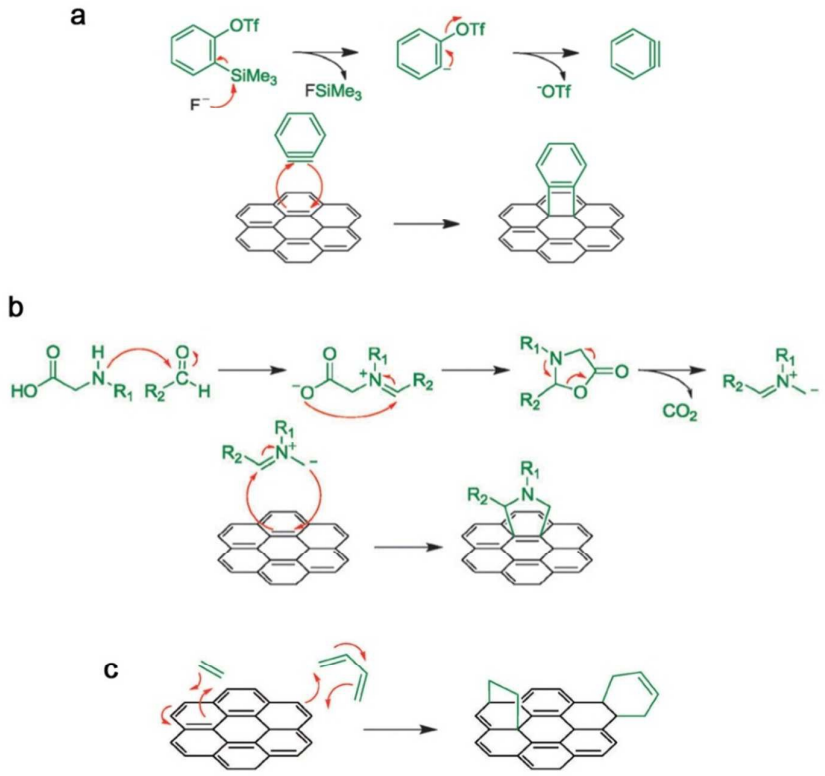

Fig. 6 (a) Mechanism of the formation of benzyne via a fluoride induced decomposition methodology (top) and the cycloaddition of graphene with benzyne (bottom). (b) Mechanism of the formation of azomethine ylide from N–methyl glycine (top) and the 1,3–Dipolar cycloaddition of graphene with azomethine ylide (bottom). (c) Mechanism of Diels–Alder cycloaddition with graphene as dienophile and diene. Reproduced from reference 45 with permission.

Furthermore, a six–membered ring can be obtained through the Diels–Alder cycloaddition, which is the most famous pericyclic reaction in organic chemistry. This [4+2] cycloaddition reaction involves the interaction between a conjugated diene and a dienophile; the overlap of the HUMO of diene and the LUMO of dienophile leads to the formation of six-membered ring(Fig. 6c).[86–87] The unsaturated dangling bonds

located on C atoms facilitate the Diels–Alder cycloaddition.[88]

1.1.6 Asymmetrical functionalization of graphene basal plane

Graphene is composed of carbon atoms that connected together by strong covalent bonds, which are predicted to be impermeable to small atoms or molecules. This property makes graphene potential for bifacially asymmetric modification. For example, Janus graphene comprises two types of functional groups separated by the single–mediated carbon layer (described as X–G–Y, Fig. 7) has been successfully synthesized.[89] In this case, a 200–300 nm thick poly(methyl methyacrylate) (PMMA) film was utilized as a flexible macroscopic mediator for a two–step functionalization. Upon the combination of photochlorination, fluorination, phenylation, diazotization and oxygenation reactions, four types of Janus graphene have been obtained by

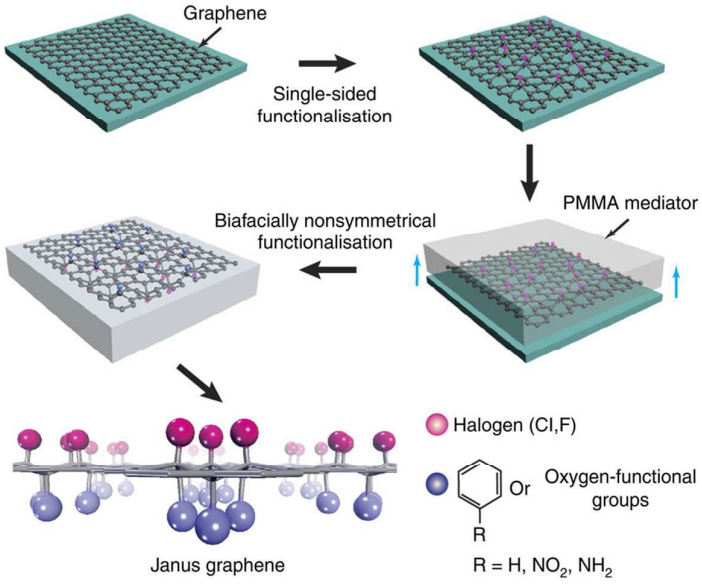

Fig. 7 Schematic illustration of the PMMA–mediated transfer procedure to fabricate Janus graphene. Reproduced from reference 89 with permission.

asymmetrically bonding X and Y atoms on both surfaces of graphene. The functionalities on one side are capable of influencing the chemical reactivity and surface wettability of the opposite side. Thus, this asymmetric structure can efficiently control the self–assembly of graphene sheets. Moreover, it has been proven that the asymmetric functionalization breaks the symmetric restriction of graphene, giving it a non–zero bandgap. The modulated bandgap linearly correlates with the binding energy difference between the two functionalities.

1.2 Functionalization of graphene edges

The edge carbons of graphene adopt tetrahedral geometries, providing them with more freedom than that of basal plane carbons without causing extra strain.[90–92] Therefore, edge carbon atoms are more reactive than those on basal plane. Graphene edges have two different configurations: "armchair" and "zigzag".[34,93] They can also have a combination of both configurations. Each carbon atom of the zigzag edge has an unpaired electron, making it easy to bond with other moieties. The carbon atoms of the armchair edge are more stable because the presence of a triple covalent bond between the open edges carbon atoms. Furthermore, the presence of edge defects in CMG facilitates chemical reactions, and provides opportunities for functionalization. The typical defect sites for functionalization include edge sites with dangling bonds, vacancies, and defect sites decorated with functional groups such as carbonyl, epoxy, and carboxyl groups.[13] The functionalization of graphene edges can improve the solubility and assembly behavior of graphene.[94,95] However, the bandgap of graphene

exhibits no obvious change, because its sp^2 network is undisturbed.[96]

1.2.1 Functionalization of pristine graphene edge sites

Under ambient conditions, the termination–free graphene edges can quickly react with adsorbed molecules. In the terminology of modern organic chemistry, the free armchair sites are the *o*–benzyne (or carbyne) type, while the free zigzag sites are the carbene type (Fig. 8).[96,97] The zigzag sites enable many carbene related reactions such as cycloaddition and insertion.[97,98] Pericyclic and insertion reactions can also be applied to armchair–edged graphene nanoribbons (GNR).[99] Recently, Diels–Alder reactions have been carried out at graphene edges, and it is becoming a powerful strategy to adjust the electronic properties of graphene under mild conditions.[86] The mechanisms of these addition reactions has already been discussed in the section of "functionalization on graphene basal plane".

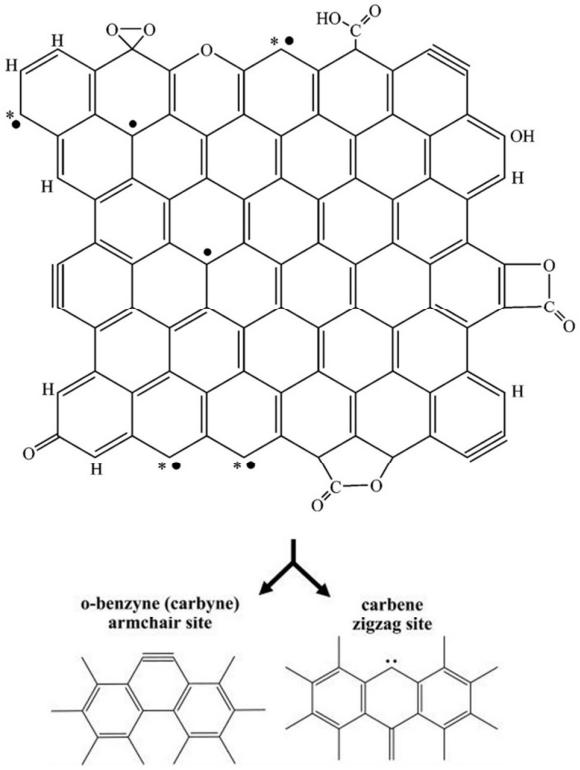

Fig. 8 Schematic representation of the main chemical features in a graphene sheet, with its typical surface functionalities, and including the free edge sites. Reproduced from reference 97 with permission.

1.2.2 Functionalization of CMG edge sites

The edge sites of CMG can be decorated with various moieties such as carbonyl, carboxylic, and hydroxyl groups. These groups facilitate CMG for further functionalization and improve the solubility of CMG in organic or aqueous solutions. The most commonly used functionalization precursor is GO, having abundant carboxyl groups at its edges (Fig. 3). Generally, the carboxyl groups of GO have to be activated through two routes: (1) Pre–treatment with $SOCl_2$; (2) Coupling with alcohol or amine.[32] These methodologies are not limited to GO; they can also be used

to activate small molecules, oligomers, polymers, and C_{60}.[100,101]

The amidation reaction of coupling carboxyl and amino groups is an effective route to modify CMGs. Amino–terminated polymers, chromophores, biomolecules, ligands have been successfully anchored onto CMG sheets by this technique.[14,102,103] Similarly, the coupling of alcoholic and carboxyl groups has also been widely used to functionalize CMGs.[104,105] An important reaction is between hydroxyl terminated poly(3-hexylthiophene) (P3HT) and GO.[101] The P3HT-grafted GO is soluble in common organic solvents, facilitating materials analysis and device fabrication via solution processing. For example, a photovoltaic device can be prepared using P3HT-grafted GO together with C_{60}. This device showed improved power conversion efficiency because of the extended electron delocalization of GO upon covalently attaching P3HT.

1.3 Noncovalent functionalization of graphene

Noncovalent functionalization usually involves decorating functional species onto graphene sheets via π–π stacking, hydrophobic attraction, hydrogen bonding and/or electrostatic interactions.[14,48,106,107] This is a physical process achieved by polymer wrapping, adsorption of surfactants or small aromatic molecules, etc (Fig. 9).[108–112] Different from the covalent functionalization, noncovalent functionalization of graphene maintains the structure and properties of graphene.

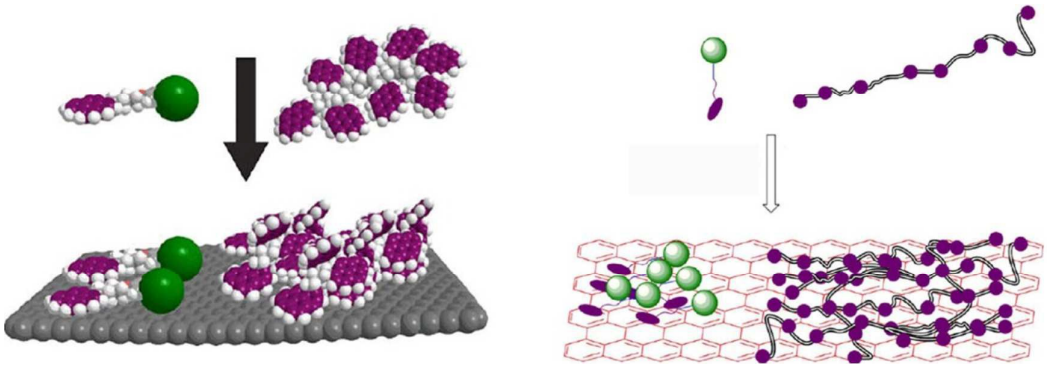

Fig. 9. Schematic of the noncovalent functionalization of graphene using polymers and small–molecules. Reproduced from reference 112 with permission.

1.3.1 Conjugated compounds

Pristine graphene and rGO are easily to form irregular aggregates in solutions because of their conjugated structures and hydrophobicity. Decorating graphene with conjugated compounds can be used to obtain stable suspensions of graphene sheets.[113–117] Generally, the conjugated compounds have polyaromatic rings and functional groups. The conjugated polyaromatic rings attach to the sp^2 network of graphene sheets via π–π stacking, and the functional moieties stabilize graphene sheets in solvents and/or provide graphene with new functionalities. Typical conjugated compounds are naphthalene, anthracene, pyrene, porphyrin and their derivatives, etc.[118] For example, 5, 10, 15, 20–Tetrakis(1–methyl–4–pyridinio) porphyrin (TMPyP) molecules can be decorated onto rGO sheets in monolayer via π –π stacking and electrostatic interactions.[119] The strong interaction between these two comments forces the molecular flatting of TMPyP molecules. The TMPyP functionalized rGO sheets can be stably dispersed in water and can be used to detect

Cd^{2+} ions rapidly and selectively.

1.3.2 Polymers

Stable dispersions of graphene sheets in various solvents can also be obtained through noncovalent functionalization with polymers. For example, amine terminated polystyrene can electrostatically interact with the carboxylate groups of rGO sheets.[110] This interaction made polystyrene chains to be coated on rGO sheets, transferring rGO sheets from an aqueous phase to an organic phase. Immobilizing biomacromolecules on graphene sheets through noncovalent functionalization has also attracted a great deal of interest.[14,32,120] The large specific surface area, excellent properties and biocompatibility of graphene extend the applications of biomacromolecules. For example, rGO sheets were decorated with amphiphilic polyethylene glycolylated (PEGylated) polymers, rendering them stable in biological systems.[103,121] Other typical biomolecules that can immobilize onto graphene sheets include enzymes, chymotrypsin, proteins and trypsin, etc. [14,122–125]

2. Doping

Chemical doping is one of the most promising techniques to tailor the electronic structure of graphene by charge injection or extraction.[27,30,31,126,127] Pristine graphene is a zero bandgap semimetal, and its Fermi level locates near the Dirac point (Fig. 12A).[127] Chemical doping is proposed to tune the bandgap by shifting the Dirac point relative to the Fermi level.[129,130] As the Dirac point is above (below) the Fermi level,

the doped graphene is a p–type (n–type) semiconductor (Fig. 10B).[128] In principle, chemical doping of graphene can be classified into two categories: surface transfer doping and substitutional doping.[27,131] Surface transfer doping is achieved by the charge transfer between graphene and the dopants adsorbed on its surface. In most cases, this route does not destroy the chemical bonds of graphene. As for substitutional doping, heteroatoms (e. g., nitrogen, boron, and sulfur atoms) replace the carbon atoms in the skeleton of graphene, disturbing its structure.

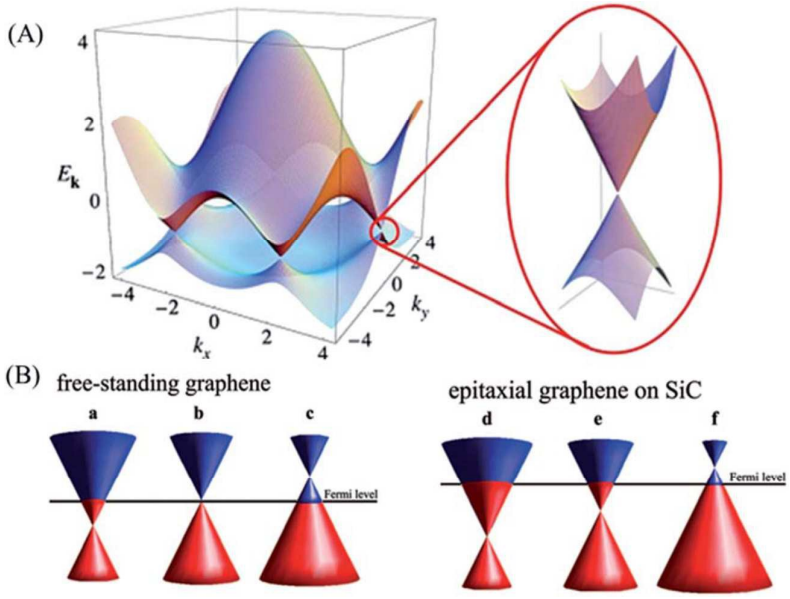

Fig. 10 (A) Left: electronic dispersion in the honeycomb lattice. Right: zoom–in of the energy bands close to one of the Dirac points. (B) A schematic diagram of the position of the Dirac point and the Fermi level as a function of doping. Left: n–type doped, pristine and p–type doped free–standing graphene (a–c). Right: n–type doped, pristine and p–type doped epitaxial graphene grown on silicon carbide (d–f). Reproduced from reference 128 with permission.

2.1 Surface transfer doping

In surface transfer doping, molecules with electron withdrawing or donating groups adsorb on the surfaces of graphene sheets, leading to the formation of p–type or n–type doped graphene. A variety of species including gases, organic molecules and metal atoms can adsorb on graphene sheets.[132–135]

P–type doped graphene can be easily formed in air or in oxygen atmosphere. Yavari *et al.* reported that the bandgap of graphene can be opened by adsorbing water on the surface of graphene sheet.[136] Strong electron acceptors, such as NO_2, Br_2, I_2, can also act as p–type dopants.[137] On the other hand, ethanol, NH_3 and CO are n–type dopants.[138]

The adsorption of organic molecules is also able to tune the bandgap of graphene. For example, Wei et al. doped graphene with 2–(2–methoxyphenyl)–1,3–dimethyl–2,3–dihydro–1*H*–benzoimidazole (*o*–MeO–DMBI). The electrical property of graphene has been changed from p–type to n–type by varying the amount of *o*–MeO–DMBI (Fig. 11).[139]

The surface of graphene can adsorb various metal atoms. On the basis of the difference between the work functions of both components, the doping types of graphene can be modulated. Upon the electron transfer to equilibrate the Fermi levels, graphene is *n*–type doped with Al, Ag and Cu, while *p*–doped with Au and Pt.[129]

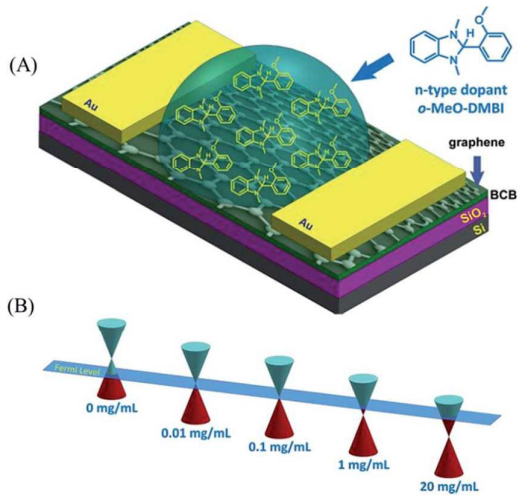

Fig. 11 (A) Chemical structure of *o*–MeO–DMBI and the schematic illustration of a *o*–MeO–DMBI doped CVD–grown graphene transistor by the solution process. (B) Schematic illustration of the shifts in the Fermi level toward the Dirac point varied with the o–MeO–DMBI solution concentration. Reproduced from reference 139 with permission.

2.2 Substitutional doping

A variety of atoms have been introduced into graphene to change its electron density and to broaden its applications. Atoms with fewer or more valence electrons than that of carbon lead to form p-doped or n-type graphene. Two chemical approaches have been developed to prepare heteroatom doped graphene: in-situ doping and post treatment. Chemical vapor deposition (CVD),[140,141] solvothermal reaction[142] and arc discharge[143] are effective techniques for in-situ doping of graphene during its growth. These techniques can produce homogeneously doped graphene materials. Post–treatment of bulk graphene materials by thermal annealing or plasma in the

atmospheres with molecules containing heteroatom possibly dopes them only on their surfaces.[144] Heteroatom doping will influence the charge distribution of carbon atoms in graphene, making the doped graphene to be a good electrode material for fabricating field effect transistor (FET) devices.[28,145] Moreover, the structural defects induced by doping in graphene are usually the active sites for surface chemical reactions. Thus, doped graphene materials frequently exhibit superior performances in catalysis and sensors.[146,147]

2.2.1 Nitrogen–doping

The nitrogen atoms (N) doped in the carbon lattice of graphene mainly has three bonding configurations: pyridinic N, pyrrolic N, and quaternary N (or graphitic N) (Fig. 12).[144,148] Specifically, pyridinic N atom bonds with two C atoms at the edges or defects of graphene. A pyridinic N oxide has one oxygen atom bonded to the pyridinic N atom. A pyrrolic N refers to the N atom bonding with two C atoms and forming a five–membered ring, like that in pyrrole. Quaternary N refers to the three N atoms

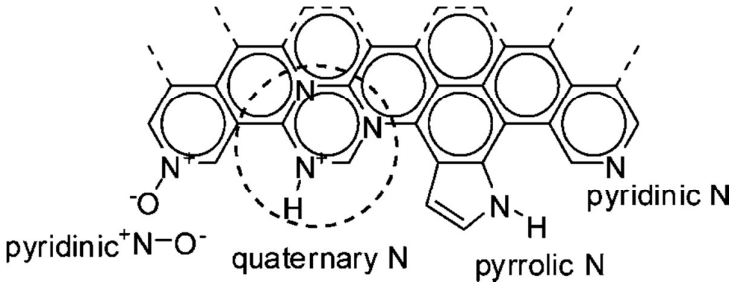

Fig. 12 Bonding configurations for nitrogen atoms in N-doped graphene. Reproduced from reference 148 with permission.

symmetrically substitute C atoms in a hexagonal ring. Among these bonding configurations, pyridinic N and quaternary N are sp^2 hybridized, and pyrrolic N is sp^3 hybridized. Pyridinic and quaternary N has marginal influence on the graphene structure.[144] In contrast, sp^3 hybridized pyrrolic N disrupts the planar structure of graphene. First-principles calculations on the reaction paths of NH_3 on graphene defects indicate that the types of defects determine the configurations of doped N atoms: graphitic-N at single vacancies, pyridinic or pyrrolic-N at divacancies, pyrrolic-N at armchair edges, and N in a four-member ring at zigzag edges.[149] Actually, N-doping can be controlled by introducing defects into graphene sheets via a physical approach (e.g. N^+-irradiation) and followed by annealing in NH_3.[150]

The electronegativity of N (3.04 on the Pauling scale) is larger than that of C (2.55 on the Pauling scale). Thus, N-doping creates polarization in the carbon network, thereby influencing the electronic, magnetic and optical properties of graphene.[151] N-doping opens a bandgap near the Dirac point, conferring graphene with semiconducting properties.[152] The semiconducting character of N-doped graphene depends on the configurations of doping atoms. For a graphitic N (Fig. 12), three valence electrons of N are bonded with the neighboring carbon atoms, one electron is engaged in a π bond formation, and the fifth electron is involved in the π^* state. Thus, N atoms contribute electrons to the graphene lattice, resulting in an n–doping effect.[153] In comparison, pyridinic and pyrrolic N atoms induce p-doping effects by withdrawing electrons from graphene sheet.[154]

N-doping can effectively tune the work function of graphene, which is useful for

FETs and (light emitting diode) LEDs. Schiros et al. calculated the work function of pristine graphene (4.43 eV) and graphene doped with graphitic N (3.98 eV), pyridinic N (4.83 eV), and hydrogenated pyridinic N (4.29 eV).[155] The changing of graphene work function is caused by the electron donating or accepting nature of each N–bonding configuration.

Pristine graphene shows magnetic hysteresis at room temperature, however, heteroatom doping can create a magnetic moment in graphene.[156] Among the doping N atoms, graphitic N (Fig. 12) is not able to generate a magnetic moment because of the lack of nonbonding electrons. For pyridinic N, the unpaired spins are localized on N atoms that concentrated at graphene edges. Hence, it has less influence on the spin polarization of the edge states. Therefore, only pyrrolic N atoms can create strong magnetic moments.[157]

N-doping can also tailor the optical properties of graphene sheets. Chiou et al. studied the influence of N-doping on the photoluminescence (PL) property of graphene.[158] Upon irradiating N atoms with lights, the electrons were excited from ground N 1s orbitals to unoccupied 2p orbitals (π* state). Then, the electrons were transferred from π* state to π state, accompanying with releasing energy in the form of PL emission. Therefore, N-doping enhances the PL emission of graphene significantly.

Large–area high–quality N-doped graphene can be prepared by CVD technique. Typically, a mixture of a carbon source gas (e.g., CH_4) and an N-containing gas (e.g., NH_3) decomposed at a metal catalyst (e.g., Cu or Ni) foil to form N-doped

graphene.[127] Liquid and solid organic precursors (e.g., pyridine, pyrazine) have also been explored for this purpose.[159,160] N-doped graphenes with high N contents can be prepared by solvothermal treat or thermal annealing GO in the presence of different N sources.[161,162]

2.2.2 Boron doped graphene

Boron ($2s^12p^1$) is the neighboring element to carbon ($2s^2p^2$) with only one less valence electron; thus it is a typical p-type dopant for graphene.[152] In-plane substitutional doping (*e.g.*, in-plane BC_3) is more stable than out-of-plane bonding (Fig. 13a).[163] As a B atom forms sp^2 hybridization in the carbon lattice, the planar structure of graphene is retained. In contrast to this graphitic bonding configuration, bonding a B atom in a vacancy will create structural distortion. Theoretical calculation suggests a new type of structural rearrangement, a tetrahedral-like BC_4 configuration that saturates all the dangling carbon atoms (Fig. 13b).[164] This B-doped configurations distorts the planar structure of graphene. B-doping induces the Fermi level of graphene downshift towards its Dirac point. Theoretical calculation indicates that a bandgap of 0.14 eV can be introduced by doping a B atom into a graphene network with 50 carbon atoms.[126]

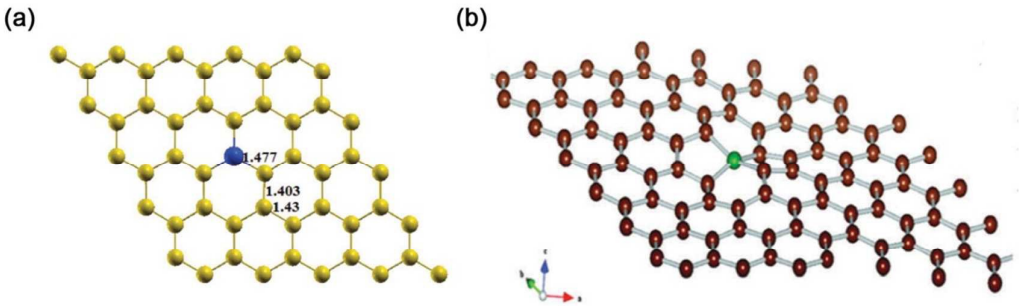

Fig. 13 (a) Substitutional doping of B (blue ball). Reproduced from reference 163 with permission. (b) B atom in a vacancy with symmetric disposition (green ball). Reproduced from reference 164 with permission.

A B-doped few-layer CVD graphene was produced by using ethanol and boron powder as the carbon and boron sources.[141] This graphene contains about 0.5 % B atoms, showing electrical features of a p-type semiconductor. Furthermore, a graphene doped with 3.5 at% B was produced via thermal annealing GO in the presence of boron oxide.[165] Compared to pristine graphene, B-doped graphene has more excellent electrocatalytic properties. The bandgap of B-doped graphene is tunable by modulating its doping level. For example, when the B content changed from 0 to 13.85% via a microwave plasma method, the bandgap of doped graphene was changed from 0 to 0.54 eV.[166] Boron doped graphene nanoribbons with widths of 7, 14 and 21 carbon atoms were synthesized by on-surface chemical reaction of an organoboron compound. The locations of doped B atoms have defined in the centres of the nanoribbons with a programmed content of 4.8 atom%. This work provided an effective approach for doping graphene with B atoms in a controllable fashion.[167]

3. Photochemistry of graphene

Chemical doping is one of the most widely used techniques to tailor the surface and electronic structure of graphene. However, the relatively inert nature of graphene is the biggest challenge for chemical functionalization, or doping graphene to a high level. Recently, photochemical reactions have been explored for addressing this issue.[168–171] A variety of photo sources including sunlight,[172] UV light,[173] and excimer laser radiation[174] have been applied to reduce the energy barriers of graphene reactions. Highly reactive chemical species can be produced under irradiation, mainly in the form of free radicals.[175,176] Photo-induced free radicals usually can overcome the high reaction barriers of graphene addition reactions. Under irradiation, the functional groups of CMG provide reactive sites for photochemical modifications, such as photoreduction[177,178] and photopatterning.[179,180]

3.1 Free radical based photochemical reactions

Chlorine (Cl) radical can be produced from Cl_2 by irradiation. Inspired by the addition reaction of chlorine and benzene to produce a well-known insecticide, hexachlorocyclohexane (C_6Cl_6), Liu et al. developed a photochemical approach to chlorinate graphene through covalently bonding chlorine radicals to the basal plane carbon atoms (Fig. 14a).[181] In this case, graphene sheets with a coverage of C–Cl bonds up to 8 atom% were formed. Because the C=C bonds of graphene were transformed from sp^2 to sp^3, the resistance of graphene increased over 4 orders of magnitude and a bandgap was created. Moreover, graphene sheets with desired

chemical patterns can be prepared by localized photochlorination (Fig. 14b), offering a feasible approach to realize all–graphene circuits. Theoretical calculations has also been used to analyze the structural and energetic changes of chlorinated graphene in the photochemical process (Fig. 14c).[182] In the initial reaction stage, photogenerated chlorine atoms tended to adsorb onto graphene to form a stable Cl-graphene charge transfer complex. The C orbitals kept sp^2 hybridization and graphene was p-type doped. Further chlorination induced the formation of two adsorption states: one is covalently bonding Cl pairs to the C atoms with a structure closing to sp^3 hybridization. Successively, it changed into a more stable configuration, the neighboring Cl atoms bonding with carbon atoms arranged in a hexagonal ring. The another sate is nonbonding. Two adjacent chlorine atoms combine with each other, forming chlorine molecules to desorb from graphene surface. The bandgap of chlorinated graphene can be tuned in the range of 0–1.3 eV by its chlorine coverage.

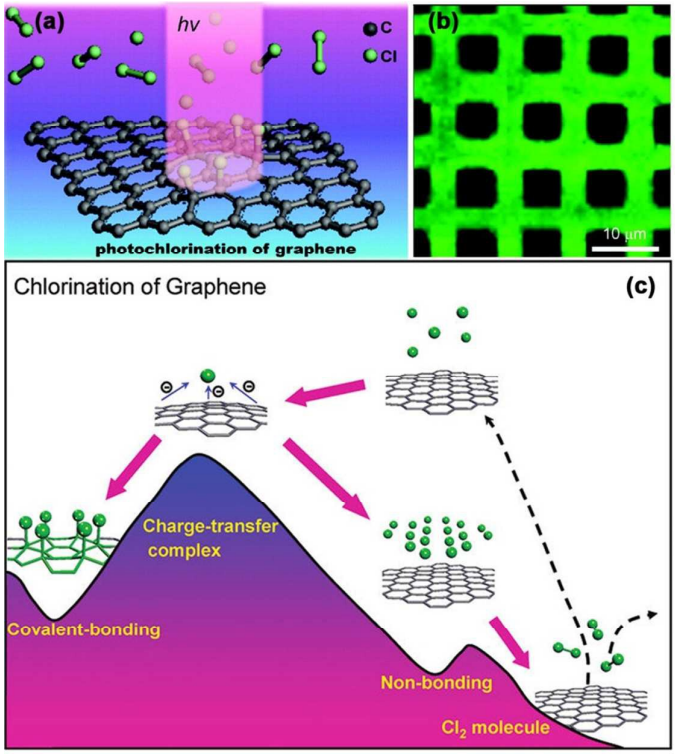

Fig. 14 (a) Schematic illustration of graphene photochlorination. (b) Raman D band mapping for a CVD–grown graphene film after a patterned photochlorination. Reproduced from reference 181 with permission. (c) Schematic diagram for the evolution of various adsorption configurations during chlorination of graphene. Reproduced from reference 182 with permission.

Fluorinated graphene has been discussed in the section of covalent functionalization. This functionalized graphene was usually prepared by F-based plasma or using XeF_2 as a reactant under harsh conditions.[183,184] Fluorinated graphene can also be produced by irradiating fluoropolymer wrapped graphene.[179] A phoexcitation with high photo flux induces scission and defluorination of fluoropolymer chains, and produces active intermediates such as CF_x and F radicals.

These radicals can react with sp^2-hybridized graphene and form C–F sp^3 bonds. Photofluorination leads to a dramatic increase in the resistance of graphene, while the basic skeletal structure of the carbon network is maintained. Furthermore, photochemical approach is environmentally friendly without releasing of unreacted toxic species.

Apart from halogenic addition reaction, alkylation reaction can also occur at the basal plane of graphene. For example, phenyl radicals can be generated by irradiation of benzyl peroxide with an Ar ion laser beam and they can react with graphene basal plane.[175] This reaction resulted in a significant decrease (50%) in electrical conductivity and an increase in hole doping level of graphene because of the introduction of the sp^3 defects and F containing moieties.

3.2 Photoreduction

Photoreduction of GO has been extensively studied because of its mild reaction condition, and it is applied to prepare graphene materials with different reduction degrees and desired patterns.[178,185–187] Even under ambient environment, the photoreduction of GO is observable by its slow colour change.[188] If replacing ambient light with a 300 W Xe lamp irradiation, the photoreduction process can be greatly shortened to be within 80 min. In the photoreduction process, the electrons in the sp^2 domains of GO sheets were partly excited (π–π^* excitation) to form electron-hole pairs. The generated electrons split off hydroxyl groups on graphene basal plane to release H_2O molecules, and reconstruct the sp^2 domains. Similarly, the epoxy groups

of GO can also be reduced by the irradiation with a 500 W high-pressure Hg lamp. In this case, the photo generated electron-hole pairs were trapped by epoxy groups.[178] The O atoms in C–O–C bonds were oxidized by the holes to form O radicals. Then, the O radicals combined into molecular O_2 and released. The oxidized carbon atoms on the graphene lattice were reduced by electrons to form sp^2 domains. After photoreduction, the conductivity of GO could be be increased by 10^5–10^7 times.

Apart from visible or UV light, laser irradiation has also been adopted for GO reduction because of its unique advantages including reliability, amenability, and the ability of arbitrary patterning.[189–191] Recently, a facile lightScribe technique has been developed for the photochemical reduction of GO. Kaner's group used a 788 nm infrared laser on a standard LightScribe DVD drive for this purpose (Fig. 15a).[190] This photoreduction was induced by photochemical and photothermal effects. Especially, the wavelength of an infrared laser is longer than those of UV and visible lights, thus the photothermal effect takes the principal role on the reduction of GO. LightScribe photoreduction can produce a large-area rGO film on a flexible substrate in a short time. Thus, it is a promising technique for rapid fabrication of graphene-based electronics. Kaner's group further patterned graphene electrodes through LightScribe reduction (Fig. 15b),[192] providing a facile pathway for electronic patterning and for developing new sensors or catalysts.

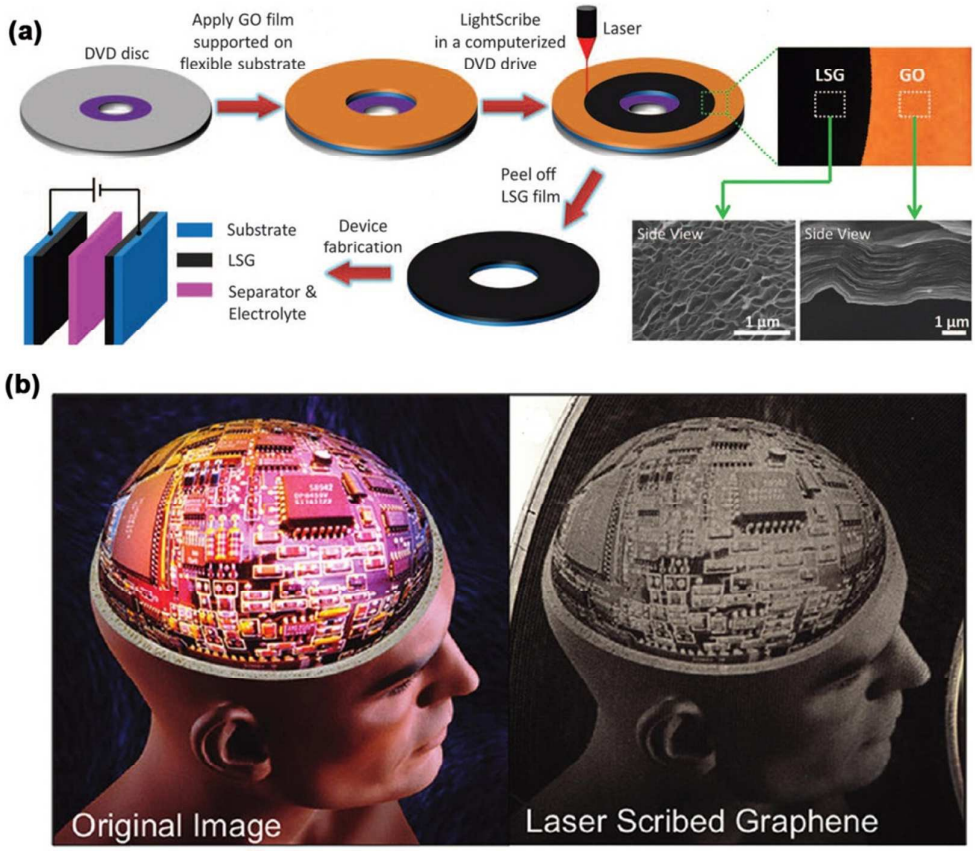

Fig. 15 (a) Schematic illustration of the fabrication of laser–scribed graphene–based electrochemical capacitors. Reproduced from reference 190 with permission. (b) Comparison between a standard complex colored image of a man's head filled with circuits and the same image reproduced by reducing graphite oxide at various levels, which corresponds to a change in electrical properties. Reproduced from reference 192 with permission.

4. Catalytic Chemistry

A graphene sheet has a fully accessible surface for adsorbing chemical moieties. However, the sp^2 hybridized pristine graphene is relatively chemically inert, showing weak catalytic activity. CMGs, doped graphene and functionalized graphene possess

structural defects (e.g. holes, structural distortions, zigzag edges), doped heteroatoms and functional moieties as catalytic sites (Fig. 16).[38] Graphene can also act as a conductive substrate with large specific surface area for immobilizing catalysts.[193–195] Here, we focus on the chemistry of graphene; thus only the inherent catalytic chemistry of graphene is discussed.

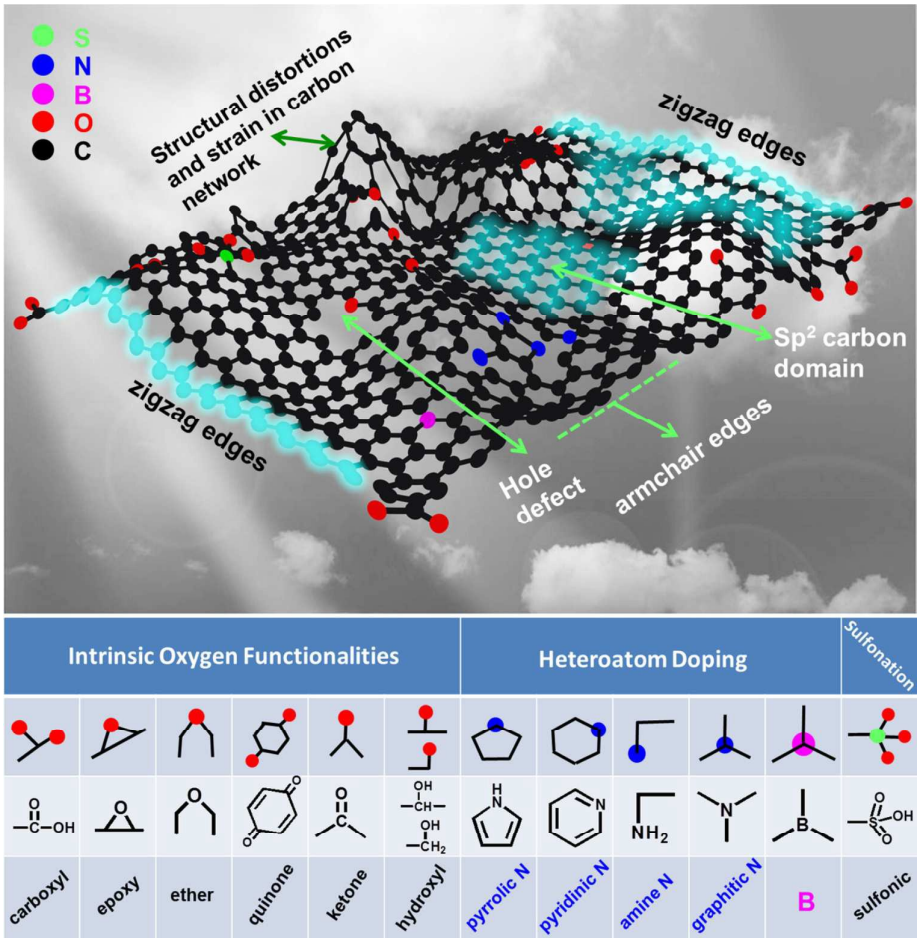

Fig. 16 General schematic model illustrating the possible active sites on graphene and its related materials for a variety of catalytic reactions. Black, red, magenta, blue and green balls represent carbon, oxygen, boron, nitrogen, and sulfur atoms, respectively. Reproduced from reference 38 with permission.

4.1 GO catalyst

The oxygen–containing groups, edges and hole defects of GO contribute to its intrinsic catalytic activity. Bielawski *et al.* reported that GO could be used as a carbocatalyst for the oxidation of alcohols and alkenes, and the hydration of alkynes.[196] These reactions occurred under relatively mild conditions with good yields. Moreover, the GO catalyst can be readily recovered by filtration. Theoretical simulations revealed that these catalytic reactions were performed via the transfer of hydrogen atoms from the organic molecules to the epoxide groups on GO basal planes. This process led to the ring–opening of the epoxide groups and dehydration of GO sheets, resulting in the formation of partially reduced GO. The partially reduced GO catalyst could be regenerated by molecular oxygen that beneficial for catalyst recycling.[197] The catalytic activity of the epoxy groups of GO has also been confirmed experimentally. Furthermore, the hydroxyl groups neighboring to the epoxy groups of GO can enhance the reaction activity of the C–H bonds of organic compounds.[198]

Apart from the band theory, an electron transfer mechanism has been proposed for explaining the intrinsic peroxidase–like activity of GO.[199] GO even showed higher activity than traditional peroxidase to catalyze the reduction of H_2O_2. It is believed that the catalytic effect was related to the electronic structures of GO. The electron transfer occurs from the valence band of GO to the lowest unoccupied molecular orbital of H_2O_2. As a result, H_2O_2 is reduced to H_2O in the presence of GO catalyst.

4.2 rGO catalyst

rGO has much better chemical tolerance and higher thermal stability than those of GO, making it to be a more stable catalyst, especially for the reactions under harsh conditions.[20,200]Although most oxygenated groups on rGO surfaces are removed, it also exhibits catalytic activity based on its conjugated π system, structural defects and functional edges. The conjugated carbon network of rGO provides both active sites for oxidants (e.g., H_2O_2) and adsorption surface for aromatic compounds (e.g., benzene). Thus, it is a good catalyst for the low-temperature oxidation of benzene to phenol.[201] rGO can also catalyse the reduction of nitrobenzene. The unsaturated carbon atoms at rGO zigzag edges were considered as the catalytic sites for this reaction, while the graphene basal plane acted as a conductor for electron transfer. rGO has also been tested to be an effective catalyst for electrochemical polymerisation,[202] ethylene hydrogenation,[41] reduction of 2,4–dinitrotoluene,[203] based on its excellent electrical conductive property and its catalytic sites of defects or carboxyl groups on edges.

4.3 Doped graphene catalyts

Doping graphene with heteroatoms (e.g., N, B, P, I and S) has proved to be an efficient method to modify the electronic structure of graphene and endow graphene with intrinsic catalytic activities.[127,204–206] N–doped graphene is a promising metal–free catalyst for oxygen reduction reaction (ORR). In the three bonding configurations of N atoms (Fig. 12), pyridinic–N atoms have been widely regarded as the active sites

of catalysis, because their delocalized p electrons facilitate the reductive adsorption of O_2 molecules. Recent studies indicated that the carbon atoms neighboring to pyridinic–N atoms had the highest spin density.[207] Thus, these carbon atoms are positively charge, providing pyridinic–N doped graphene with a strong catalytic activity for ORR.[208] Furthermore, the graphitic–N atoms in the carbon lattice facilitate the electron transfer from the carbon conductive bands to the antibonding orbitals of O_2,[209] enhancing the ORR catalytic activity of N–doped graphene. Therefore, both pyridinic and graphitic N atoms contribute to the catalytic performance, while playing different roles.

In comparison with solely atom doped graphene, co-doped graphene usually exhibit stronger catalytic activities.[210] For example, N, S dual–doped graphene was tested to be an ORR catalyst with catalytic performance comparable to that of commercial Pt/C, significantly stronger than that of N- or S-doped graphene.[211] The dual activation of C atoms is responsible to the high–activity of this catalyst as evidenced by both experiments and theoretical stimulations. Theoretical calculation indicates that the maximum spin density of N, S co–doped graphene (0.42) is much higher than that of N–doped (0.03) or S–doped graphene (0.16). In the catalytic chemistry, spin density directly related to the charge density of active sites, determining the activity of catalyst. Furthermore, the co–doping of S and N atoms introduces asymmetrical spin and charge distributions, making the number of active C atoms in co-doped graphene much more than that in sole atom doped–graphene.

Functionalized graphene catalysts

The feasibility of graphene functionalization provides abundant possibilities to develop new graphene based catalysts. Graphene network acts as a substrate for the attachment of functional groups, and provides highly conductive pathways for electron transfer. For example, sulfonated graphene were explored as solid catalysts for acid catalyzed liquid reaction,[212] ester–exchange reaction,[39] and esterification reaction.[213] A hydrogenated graphene was also reported be an effective catalyst for oxidation of organic dye.[52] The defects and sp^3 hybridized carbon atoms on the hydrogenated graphene facilitated the splitting of H_2O_2 into hydroxyl radicals to react with dyes.

5. Supramolecular chemistry

In the above sections, we mainly focus on graphene chemistry at atom level. However, the molecular behavior of graphene is important for the design and the fabrication of graphene materials with practical importance. CMGs can be regarded as 2-dimensional conjugated macromolecules with huge molar masses. GO sheets behave like amphiphilic molecules with hydrophilic edges and more hydrophobic basal planes. rGO is hydrophobic, however, it can be chemically modified through covalent or non–covalent approaches.[42] Chemically modified rGO exhibits molecular properties like GO. The supramolecular behavior of CMG sheets provides many opportunities to construct macroscopic architectures from nano-building blocks.

5.1 Liquid crystals

Liquid crystal (LC) is a supramolecular behavior of ordering molecular building blocks in fluid state. In the theoretical frame of colloidal LCs, 2D topological nanoplatelets with high asymmetry should form lyotropic LCs above a critical concentration (CC). Pristine graphene sheets can form LCs in chlorosulfonic acid at concentrations > 1.8 mg cm^{-3}.[214] Pristine graphene sheets tend to stack together driven by π–π interaction. However, in chlorosulfonic acid, graphene sheets were were protonated to bring positive charges, enhancing their repulsion force and decreasing the tendency of stacking. As a result, protonated graphene dispersions formed isotropic rigid phases at high concentrations. Under a cross–polarizer, these rigid phases showed fingerprint–like textures, typical for LCs.

GO dispersions with concentrations higher than their CCs can also form LCs, driving by the competition between orientation entropy and excluded volume entropy. Typically, GO sheets in an aqueous dispersion start to form a partial ordered structure at the concentration around 3 mg cm^{-3}, forming stable nematic mesophases at 5–8 mg cm^{-3} and high-level lamellar mesophase at concentrations >10 mg cm^{-3} (Fig. 17).[215–217] Further increasing GO concentration to 0.38 vol% (mass density ~13.2 mg cm^{-3}) following the nematic phase of 0.23 vol% (mass density ~ 8 mg cm^{-3}), a new chiral liquid crystal formed.[215] This new mesophase presented a fingerprint–like texture with aligned bands, indicating the regular rotation of director vectors. Thus, the chiral mesophase behaved a quasi–long–range lamellar ordering, the interlayer spacing decreased from 112.2 to 32.7 nm as the concentration of GO increased from

0.38 to 2.12 vol%. The chiral liquid crystalline behavior is mainly based on the electronic repulsive interactions between GO sheets; therefore, it could form a twisting state of adjoining sheets boundaries.

Both the sizes and size distribution of GO sheets are key factors to determine their behavior of forming LCs: the larger GO sheets with higher aspect ratios have lower critical concentrations to form LCs or to occur mesophase transformations; a narrower size distribution leads to a narrower concentration range of phase transition and more regular alignment.[218] This guidance is useful to prepare graphene LCs with low concentrations and viscosities, beneficial for preparing macroscopic materials via wet approaches. For example, high–quality graphene fibers can be prepared by wet spinning the GO LCs.[216]

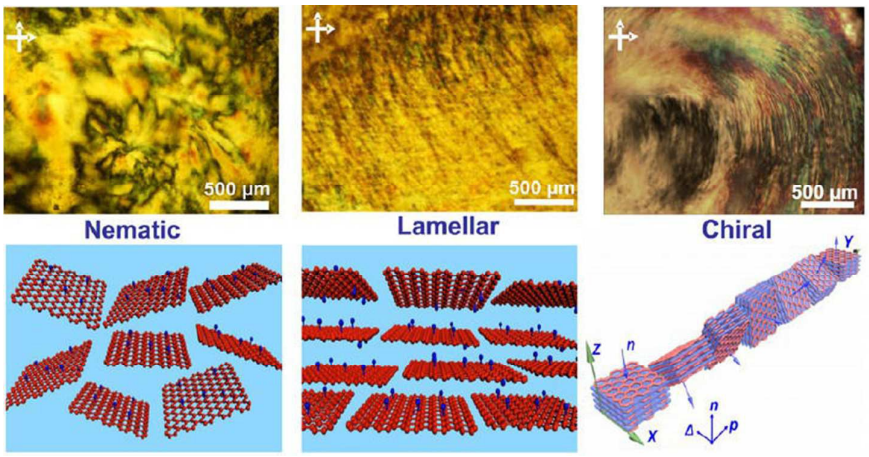

Fig. 17 Typical optical textures of GO LCs (nematic, lamellar, and chiral mesophases) and their corresponding structure models. Reproduced from reference 217 with permission.

5.2 Self-assembly

Unlike pristine graphene, CMG sheets can be readily dispersed in various solvents. The self-assembly of CMG sheets is mainly performed by their self-concentration at various interfaces, including liquid–air, liquid–liquid and liquid–solid interfaces.[44,219,220] The assembly at 2D interfaces leads to form membranes, while the assembly within 3D spaces usually produce porous 3D architectures.

5.2.1 Langmuir–Blodgett (LB) Self–assembly

LB is a technique to make molecular monolayers floating at the air-water interfaces. Typically, amphiphilic molecules were first dissolved in a volatile organic solvent, and then spread onto the water surface.[43] Upon evaporating solvent, the solute molecules were trapped on water surface, forming a monolayer. A moving barrier was used to narrow the area of the monolayer, thus effectively changed the intermolecular distance. As the film was compressed, the monolayer undergone phase transitions from gas to liquid, and then to solid before collapsing into a multilayer. The film can be transferred to a solid substrate forming a monolayer coating over a large area.

GO sheets are amphiphilic; thus they can float on water surface to form a stable monolayer without any additives. Even under a high compress force, GO layer tends to fold into wrinkles rather than collapsing into multilayers. GO sheets can be pushed together in edge-to-edge mode by compression. Overcompression may lead to a face-to-face interaction, forcing the GO sheets to slide and forming a regionally overlapped structure. Multilayered GO films can be prepared by repeatedly

transferring GO monolayers onto a flat solid substrate.

Flow directed self-assembly

Flow directed self-assembly (typically filtration) is a technique widely used for separating suspended substances from liquids. In a typical filtration process, GO sheets were self-assembled into a layered structure at the filter-suspension interface, yielding a freestanding membrane upon drying.[221] The surfaces of GO sheets are perpendicular to the flow direction, and the vacuum condition pushed GO sheets to compactly stack together. The strong intermolecular interactions between GO sheets interlocked them in a near parallel fashion. These intermolecular forces include π–stacking, hydrogen bonding and hydrophobic interactions. After drying, the water molecules between GO sheets were partly wiped off, making the as-obtained GO paper-like membrane to be mechanically strong, stiff and flexible. GO papers can be converted to conductive rGO papers by reduction.[222–224] Moreover, the flow directed self-assembly technique is easily to control the thickness of CMG paper by adjusting the volume and concentration of CMG dispersion.

5.2.2 3D Self–assembly

The self–assembly of CMG sheets in solutions has been extensively studied.[42,225,226] GO hydrogels can be prepared by increasing the binding force or decreasing the repulsion force between GO sheets in their aqueous solutions. We reported a GO/PVA supramolecular hydrogel by simply blending both components.[225] In this hydrogel,

PVA chains act as physical crosslinkers through hydrogen bonding with GO sheets to construct 3D supramolecular networks. This GO/PVA hydrogel exhibited pH induced gel-sol transition. The increasing of pH value caused further ionization of the carboxyl groups on GO sheets; therefore, the electrostatic repulsion force between GO sheets was enhanced. As a result, a gel-sol transition of the hydrogel occurred because of an insufficient binding force between GO sheets. Inspired by this work, a variety of CMG hydrogels have been prepared by us and other groups following similar procedures.[227–231] These CMG hydrogels were prepared by acidification or using small organic molecules, polymers, or ions as crosslinkers. The driving forces for self-assembling CMG sheets into 3D networks include hydrogen bonding, electrostatic and hydrophobic interactions.[232]

We developed a one-step hydrothermal method to prepare rGO hydrogels from GO dispersions without adding any crosslinkers (Fig. 18).[226] Before hydrothermal reduction, GO sheets were randomly dispersed in water and in extended states, mainly due to their strong hydrophilicity and electrostatic repulsion effect. They became regionally hydrophobic during hydrothermal process because of partially restoring their conjugated domains and removing oxygenated functionalities. The combination of hydrophobic and π–π interactions caused a 3D random stacking of flexible rGO sheets to construct a stable network. The pore sizes of the 3D rGO network are in the range of submicrometers to several micrometers. Simultaneously, the residual oxygenated functional groups on rGO sheets led to entrap ample water into the pores under high temperature and pressure to form a self-assembled graphene hydrogel. The

self-assembly of rGO sheets strongly depends the concentration, the size and size distribution of their GO precursor. The critical gelation concentration (CGC) of the GO prepared by Hummers method was tested to be around 2 mg mL^{-1} for forming a mechanically stable rGO hydrogel. The CGC decreases with the increase of GO sizes. Narrowing the size distribution of GO sheets can improve the uniformity of the pores in rGO hydrogel.

The hydrothermal process described above opened a door to prepare various macroscopic graphene materials with 3D porous frameworks including hydrogels, aerogels and foams for various applications.[233–238] However, it is energy consuming and difficult to be scaled up. To adresss these issues, we developed chemical and electrochemical reduction techniques to construct 3D rGO achitechtures. For example, self-assembled rGO hydrogel has been prepared by reducing GO dispersion with sodium ascorbate.[239] This hydrogel is electrically conductive, mechanically strong and thermally stable. It has been used as an electrode material of electrochemcal capacitors.[239,240] Electrochemical reduction of GO dispersions can deposite large-area porous rGO films on metallic electrodes.[241] The pores interconnect with each other and fully expose to electrolytes or reactants. These rGO modified electrodes have been applied for fabricating high-performance biosensors[242] and ultra-rapid electrochemical capacitors,[241] and for developing new catalyts for electrochemical oxidation of water.[243]

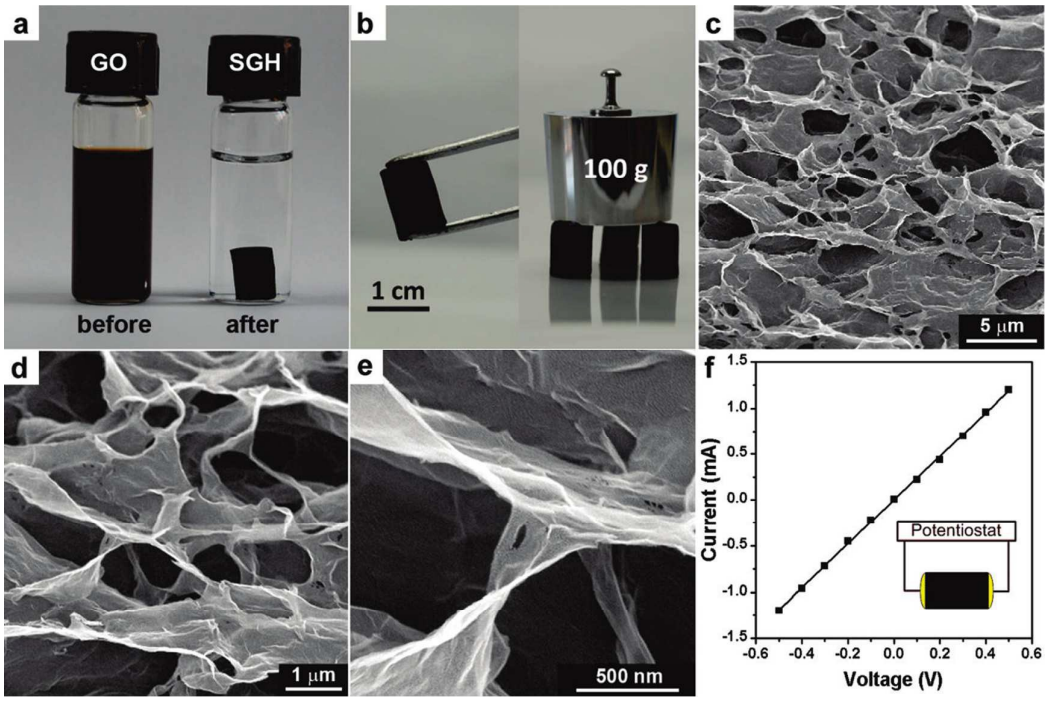

Fig. 18. (a) Photographs of a 2 mg mL^{-1} homogeneous GO aqueous dispersion before and after hydrothermal reduction at 180 °C for 12 h; (b) photographs of a strong SGH allowing easy handling and supporting weight; (c–e) SEM images with different magnifications of the SGH interior microstructures; (f) room temperature I–V curve of the SGH exhibiting Ohmic characteristic, inset shows the two–probe method for the conductivity measurements. Reproduced from reference 226 with permission.

6. Conclusion and perspective

Graphene and its derivatives are chemically active and can occur a variety of chemical reactions. These reactions are partly shared by other carbon nanomaterials such as CNTs, activated carbon and carbon black. However, the atom–thick 2D structure, large specific surface area and excellent properties make graphene sheets have chemical behaviors different from those of other nanocarbons, particularly their

asymmetric modification, and unique and attractive supramolecular chemistry. This perspective highlights the chemistry of graphene and its derivatives, including functionalization, doping, photochemistry, catalytic chemistry and supramolecular chemistry. The first four categories are mainly based on the atoms and electrons of graphene sheets, and the last category is focused on the molecular behavior of graphene derivatives.

The chemistry of graphene has been studied for only a relatively short time; thus, many chemical reactions of graphene still cannot be precisely controlled and their mechanisms have not yet been clearly revealed. For example, defect–induced chemical reactions occur either on the basal planes or at the edges of graphene sheets simultaneously. It is a challenge to establish a technique that can control the reactions within selected regions of a graphene sheet.

The accurate modulation of the bandgap of graphene is another challenge. Although several approaches have been developed for opening the bandgap of graphene, the accuracy of modulating the bandgap of graphene is still unsatisfactory. The bandgap of graphene can be tuned by changing its electronic structure through atom rearrangement of its sp^2 conjugated carbon network. However, the chemical approaches such as functionalization, doping and photochemical reactions rarely can control the compositions and structures of graphene sheets at atomic level.

The electronic structures of graphene sheets have been studied theoretically by using ideal models. However, the theoretical results frequently cannot be confirmed experimentally because of lacking perfect samples. The quality of CVD graphene and

CMGs needs further improvements by precisely controlling their compositions, defects, layer numbers and sheet sizes, etc.

CMG sheets are unique atom–thick two–dimensional building blocks and they can be assembled into fibres, membranes, and 3D frameworks. However, the microstructures and properties of these macroscopic materials strongly depend on the sizes, shapes, and functional groups of CMG sheets as well as the conditions of self–assembly. Therefore, the supramolecular chemistry of CMG sheets needs to be systematically studied.

Nevertheless, understanding the chemistry of graphene is important for designing and preparing graphene materials, and developing their practical applications. Accompanying with the technical breakthroughs in graphene production and characterizations, we believe the chemistry of graphene will be extensively investigated to provide new knowledge in the field of material chemistry.

Acknowledgements

This work was supported by the National Basic Research Program of China (973 Program, 2012CB933402, 2013CB933001), Natural Science Foundation of China (51433005).

Notes and references

1 K. S. Novoselov, V. I. Fal'ko, L. Colombo, P. R. Gellert, M. G. Schwab and K. Kim, *Nature*, 2012, **490**, 192–200.

2 M. J. Allen, V. C. Tung and R. B. Kaner, *Chem. Rev.*, 2010, 110, 132–145.

3 K. Rana, J. Singh and J.–H. Ahn, *J. Mater. Chem. C*, 2014, **2**, 2646–2656.

4 D. Wei, B. Wu, Y. Guo, G. Yu and Y. Liu, *Acc. Chem. Res.*, 2013, **46**, 106–115.

5 G. Zhou, F. Li and H.–M. Cheng, *Energy Environ. Sci.*, 2014, **7**, 1307–1338.

6 X. L. Wang and G. Q. Shi, *Energy Environ. Sci.*, 2015, **8**, 790–823.

7 H. Tian, Y. Shu, Y.–L. Cui, W.–T. Mi, Y. Yang, D. Xie and T.–L. Ren, *Nanoscale*, 2014, **6**, 699–705.

8 S. Wu, Q. He, C. Tan, Y. Wang and H. Zhang, *Small*, 2013, **9**, 1160–1172.

9 L. Kong and W. Chen, *Adv. Mater.*, 2014, **26**, 1025–1043.

10 J. Kim, J.–H. Jeon, H.–J. Kim, H. Lim and I.–K. Oh, *ACS Nano*, 2014, **8**, 2986–2997.

11 H. Sun, X. You, J. Deng, X. Chen, Z. Yang, J. Ren and H. Peng, *Adv. Mater.*, 2014, **26**, 2868–2873.

12 Q. Wu, Y. X. Xu, Z. Y. Yao, A. R. Liu and G. Q. Shi, *ACS Nano*, 2010, **4**, 1963–1970.

13 S. Eigler and A. Hirsch, *Angew. Chem. Int. Ed.*, 2014, **53**, 7720–7738.

14 Y. X. Xu, H. Bai, G. W. Lu, C. Li and G. Q. Shi, *J. Am. Chem. Soc.*, 2008, **130**, 5856–5857.

15 L. Yan, Y. B. Zheng, F. Zhao, S. Li, X. Gao, B. Xu, P. S. Weiss and Y. Zhao, *Chem. Soc. Rev.*, 2012, **41**, 97–114.

16 J. C. Meyer, A. K. Geim, M. I. Katsnelson, K. S. Novoselov, T. J. Booth and S. Roth, *Nature*, 2007, **446**, 60–63.

17 M. Ishigami, J. H. Chen, W. G. Cullen, M. S. Fuhrer and E. D. Williams, *Nano Lett.*, 2007, **7**, 1643–1648.

18 A. Fasolino, J. H. Los and M. I. Katsnelson, *Nat. Mater.*, 2007, **6**, 858–861.

19 A. K. Geim and K. S. Novoselov, *Nat. Mater.*, 2007, **6**, 183–191.

20 C. C. Huang, C. Li and G. Q. Shi, *Energy Environ. Sci.*, 2012, **5**, 8848–8868.

21 L. Kong, A. Enders, T. S. Rahman and P. A. Dowben, *J. Phys.–Condens. Mat.*, 2014, **26**, 443001.

22 M. Quintana, E. Vazquez and M. Prato, *Acc. Chem. Res.*, 2013, **46**, 138–148.

23 J. Park and M. D. Yan, *Acc. Chem. Res.*, 2013, **46**, 181–189.

24 J. E. Johns and M. C. Hersam, *Acc. Chem. Res.*, 2013, **46**, 77–86.

25 X. Gao, Z. Wei, V. Meunier, Y. Sun and S. B. Zhang, *Chem. Phys. Lett.*, 2013, **555**, 1–6.

26 E. Bekyarova, S. Sarkar, F. Wang, M. E. Itkis, I. Kalinina, X. Tian and R. C. Haddon, *Acc. Chem. Res.*, 2013, **46**, 65–76.

27 W. Zhang, L. Wu, Z. Li and Y. Liu, *RSC Adv.*, 2015, **5**, 49521–49533.

28 U. Bangert and R. Zan, *Int. Mater. Rev.*, 2015, **60**, 133–149.

29 Y. Wen, C. Huang, L. Wang and D. Hulicova–Jurcakova, *Chin. Sci. Bull.*, 2014, **59**, 2102–2121.

30 B. W. Yao, C. Li, J. Ma and G. Q. Shi, *Phys. Chem. Chem. Phys.,* 2015, **17,** 19538–19545

31 C. N. R. Rao, K. Gopalakrishnan and A. Govindaraj, *Nano Today*, 2014, **9**, 324–343.

32 D. R. Dreyer, A. D. Todd and C. W. Bielawski, *Chem. Soc. Rev.*, 2014, **43**, 5288–5301.

33 X. Zhang, J. Xin and F. Ding, *Nanoscale*, 2013, **5**, 2556–2569.

34 S. Fujii and T. Enoki, *Acc. Chem. Res.*, 2013, **46**, 2202–2210.

35 M. Minella, M. Demontis, M. Sarro, F. Sordello, P. Calza and C. Minero, *J. Mater. Sci.*, 2015, **50**, 2399–2409.

36 S. Sarkar, S. Niyogi, E. Bekyarova and R. C. Haddon, *Chem. Sci.*, 2011, **2**, 1326–1333.

37 D. R. Dreyer, H. P. Jia and C. W. Bielawski, *Angew. Chem. Int. Ed.*, 2010, **49**, 6813–6816.

38 H. Hu, J. H. Xin, H. Hu, X. Wang and Y. Kong, *Appl. Catal. A–Gen.*, 2015, **492**, 1–9.

39 L. Wang, D. Wang, S. Zhang and H. Tian, *Catal. Sci. Technol.*, 2013, **3**, 1194–1197.

40 B. Frank, R. Blume, A. Rinaldi, A. Trunschke and R. Schlogl, *Angew. Chem. Int. Ed.*, 2011, **50**, 10226–10230.

41 T. I. Perhun, I. B. Bychko, A. I. Trypolsky and P. E. Strizhak, *Theor. Exp. Chem.*, 2013, **48**, 367–370.

42 Y. X. Xu and G. Q. Shi, *J. Mater. Chem.*, 2011, **21**, 3311–3323.

43 L. J. Cote, F. Kim and J. X. Huang, *J. Am. Chem. Soc.*, 2009, **131**, 1043–1049.

44 J. M. MacLeod and F. Rosei, *Small*, 2014, **10**, 1038–1049.

45 C. K. Chua and M. Pumera, *Chem. Soc. Rev.*, 2013, **42**, 3222–3233.

46 S. T. Pantelides, Y. Puzyrev, L. Tsetseris and B. Wang, *MRS Bull.*, 2012, **37**, 1187–1194.

47 V. Georgakilas, M. Otyepka, A. B. Bourlinos, V. Chandra, N. Kim, K. C. Kemp, P. Hobza, R. Zboril and K. S. Kim, *Chem. Rev.*, 2012, **112**, 6156–6214.

48 L. Dai, *Acc. Chem. Res.*, 2013, **46**, 31–42.

49 Y. G. Zhou, Z. G. Wang, P. Yang, X. Sun, X. T. Zu and F. Gao, *J. Phys. Chem. C*, 2012, **116**, 5531–5537.

50 M. Pumera and C. H. A. Wong, *Chem. Soc. Rev.*, 2013, **42**, 5987–5995.

51 L. Reatto, D. E. Galli, M. Nava and M. W. Cole, *J. Phys.–Condens. Mat.*, 2013, **25**, 443001.

52 Y. Zhao, W. F. Chen, C. F. Yuan, Z. Y. Zhu and L. F. Yan, *Chinese J Chem Phys*, 2012, **25**, 335–338.

53 N. P. Guisinger, G. M. Rutter, J. N. Crain, P. N. First and J. A. Stroscio, *Nano Lett.*, 2009, **9**, 1462–1466.

54 Z. Q. Luo, T. Yu, K. J. Kim, Z. H. Ni, Y. M. You, S. Lim, Z. X. Shen, S. Z. Wang and J. Y. Lin, *ACS Nano*, 2009, **3**, 1781–1788.

55 D. Yu and F. Liu, *Nano Lett.*, 2007, **7**, 3046–3050.

56 D. C. Elias, R. R. Nair, T. M. G. Mohiuddin, S. V. Morozov, P. Blake, M. P. Halsall, A. C. Ferrari, D. W. Boukhvalov, M. I. Katsnelson, A. K. Geim and K. S. Novoselov, *Science*, 2009, **323**, 610–613.

57 H. Sahin, O. Leenaerts, S. K. Singh and F. M. Peeters, *Wires. Comput. Mol. Sci.*, 2015, **5**, 255–272.

58 S. Lebegue, M. Klintenberg, O. Eriksson and M. I. Katsnelson, *Phys. Rev. B*, 2009, **79**, 245117.

59 D. K. Samarakoon, Z. Chen, C. Nicolas and X.–Q. Wang, *Small*, 2011, **7**, 965–969.

60 A. H. Castro Neto and F. Guinea, *Phys. Rev. Lett.*, 2009, **103**, 026804.

61 M. Topsakal, S. Cahangirov and S. Ciraci, *Appl. Phys. Lett.*, 2010, **96**, 091912.

62 J. T. Robinson, J. S. Burgess, C. E. Junkermeier, S. C. Badescu, T. L. Reinecke, F. K. Perkins, M. K. Zalalutdniov, J. W. Baldwin, J. C. Culbertson, P. E. Sheehan and E. S. Snow, *Nano Lett.*, 2010, **10**, 3001–3005.

63 *Nano Res.*, 2011, **4**, 143–152.

64 R. R. Nair, W. Ren, R. Jalil, I. Riaz, V. G. Kravets, L. Britnell, P. Blake, F. Schedin, A. S. Mayorov, S. Yuan, M. I. Katsnelson, H.–M. Cheng, W. Strupinski, L. G. Bulusheva, A. V. Okotrub, I. V. Grigorieva, A. N. Grigorenko, K. S. Novoselov and A. K. Geim, *Small*, 2010, **6**, 2877–2884.

65 R. Zbořil, F. Karlický, A. B. Bourlinos, T. A. Steriotis, A. K. Stubos, V. Georgakilas, K. Šafářová, D. Jančík, C. Trapalis and M. Otyepka, *Small*, 2010, **6**, 2885–2891.

66 H. Şahin, M. Topsakal and S. Ciraci, *Phys. Rev. B*, 2011, **83**, 115432.

67 O. Leenaerts, H. Peelaers, A. D. Hernandez–Nieves, B. Partoens and F. M. Peeters, *Phys. Rev. B*, 2010, **82**, 195436.

68 K. S. Subrahmanyam, S. R. C. Vivekchand, A. Govindaraj and C. N. R. Rao, *J. Mater. Chem.*, 2008, **18**, 1517–1523.

69 W. S. Hummers and R. E. Offeman, *J. Am. Chem. Soc.*, 1958, **80**, 1339–1339.

70 B. C. Brodie, *Ann. Chim. Phys.*, 1860, **59**, 466–472.

71 L. Staudenmaier, *Ber. Dtsch. Chem. Ges.*, 1898, **31**, 1481–1487.

72 M. J. Hudson, F. R. Hunter–Fujita, J. W. Peckett and P. M. Smith, *J. Mater. Chem.*, 1997, **7**, 301–305.

73 J. W. Peckett, P. Trens, R. D. Gougeon, A. Pöppl, R. K. Harris and M. J. Hudson, *Carbon*, 2000, **38**, 345–353.

74 L. Y. Jiao, L. Zhang, X. R. Wang, G. Diankov and H. J. Dai, *Nature*, 2009, **458**, 877–880.

75 D. V. Kosynkin, A. L. Higginbotham, A. Sinitskii, J. R. Lomeda, A. Dimiev, B. K. Price and J. M. Tour, *Nature*, 2009, **458**, 872–875.

76 A. Lerf, H. He, M. Forster and J. Klinowski, *J. Phys. Chem. B*, 1998, **102**, 4477–4482.

77 W. W. Cai, R. D. Piner, F. J. Stadermann, S. Park, M. A. Shaibat, Y. Ishii, D. X. Yang, A. Velamakanni, S. J. An, M. Stoller, J. H. An, D. M. Chen and R. S. Ruoff, *Science*, 2008, **321**, 1815–1817.

78 D. W. Boukhvalov and M. I. Katsnelson, *J. Am. Chem. Soc.*, 2008, **130**, 10697–10701.

79 A. Nourbakhsh, M. Cantoro, A. V. Klekachev, G. Pourtois, T. Vosch, J. Hofkens, M. H. van der Veen, M. M. Heyns, S. De Gendt and B. F. Sels, *J. Phys. Chem. C*, 2011, **115**, 16619–16624.

80 M. B. Smith and J. March, *March's Advanced Organic Chemistry: Reactions,*

Mechanisms, and Structure, John Wiley & Sons, New Jersey, 2007.

81 E. Bekyarova, M. E. Itkis, P. Ramesh, C. Berger, M. Sprinkle, W. A. de Heer and R. C. Haddon, *J. Am. Chem. Soc.*, 2009, **131**, 1336–1337.

82 J. R. Lomeda, C. D. Doyle, D. V. Kosynkin, W. F. Hwang and J. M. Tour, *J. Am. Chem. Soc.*, 2008, **130**, 16201–16206.

83 J. Clayden, N. Greeves, S. Warren and P. Wothers, *Organic Chemistry*, Oxford University Press, Oxford, 2001.

84 H. F. Bettinger, *Chem.–Eur. J.*, 2006, **12**, 4372–4379.

85 J. Choi, K.–j. Kim, B. Kim, H. Lee and S. Kim, *J. Phys. Chem. C*, 2009, **113**, 9433–9435.

86 S. Sarkar, E. Bekyarova, S. Niyogi and R. C. Haddon, *J. Am. Chem. Soc.*, 2011, **133**, 3324–3327.

87 Z. Ji, J. Chen, L. Huang and G. Q. Shi, *Chem. Commun.*, 2015, **51**, 2806–1809.

88 S. J. Altenburg, M. Lattelais, B. Wang, M.-L. Bocquet and R. Berndt, *J. Am. Chem. Soc.*, 2015, **137**, 9452–9458.

89 L. Zhang, J. Yu, M. Yang, Q. Xie, H. Peng and Z. Liu, *Nat. Commun.*, 2013, **4**, 1443.

90 D. Jiang, B. G. Sumpter and S. Dai, *J. Chem. Phys.*, 2007, **126**, 134701.

91 Y. Lu, R. Wu, L. Shen, M. Yang, Z. Sha, Y. Cai, P. He and Y. Feng, *Appl. Phys. Lett.*, 2009, **94**, 122111.

92 T. Enoki and K. Takai, *Solid State Commun.*, 2009, **149**, 1144–1150.

93 M. Acik and Y. J. Chabal, *Jpn. J. Appl. Phys.*, 2011, **50**, 070101.

94 A. E. R. Castillo and G. VanáTendeloo, *Chem. Commun.*, 2011, **47**, 9330–9332.

95 D. Boukhvalov and M. Katsnelson, *Nano Lett.*, 2008, **8**, 4373–4379.

96 X. Jia, J. Campos–Delgado, M. Terrones, V. Meunier and M. S. Dresselhaus, *Nanoscale*, 2011, **3**, 86–95.

97 L. R. Radovic and B. Bockrath, *J. Am. Chem. Soc.*, 2005, **127**, 5917–5927.

98 D. E. Jiang, B. G. Sumpter and S. Dai, *J. Chem. Phys.*, 2007, **126**, 134701.

99 E. F. Sheka and L. A. Chernozatonskii, *Int. J. Quantum Chem*, 2010, **110**, 1938–1946.

100 H. Q. Bao, Y. Z. Pan, Y. Ping, N. G. Sahoo, T. F. Wu, L. Li, J. Li and L. H. Gan, *Small*, 2011, **7**, 1569–1578.

101 D. S. Yu, Y. Yang, M. Durstock, J. B. Baek and L. M. Dai, *ACS Nano*, 2010, **4**, 5633–5640.

102 S. Mallakpour, A. Abdolmaleki and S. Borandeh, *Appl. Surf. Sci.*, 2014, **307**, 533–542.

103 Z. Liu, J. T. Robinson, X. M. Sun and H. J. Dai, *J. Am. Chem. Soc.*, 2008, **130**, 10876–10877.

104 N. A. Kumar, H. J. Choi, Y. R. Shin, D. W. Chang, L. M. Dai and J. B. Baek, *ACS Nano*, 2012, **6**, 1715–1723.

105 R. Devi, G. Prabhavathi, R. Yamuna, S. Ramakrishnan and N. K. Kothurkar, *Journal Of Chemical Sciences*, 2014, **126**, 75–83.

106 T. Kuila, S. Bose, A. K. Mishra, P. Khanra, N. H. Kim and J. H. Lee, *Prog. Mater Sci.*, 2012, **57**, 1061–1105.

107 X. An, T. J. Simmons, R. Shah, C. Wolfe, K. M. Lewis, M. Washington, S. K. Nayak, S. Talapatra and S. Kar, *Nano Lett.*, 2010, **10**, 4295–4301.

108 S. Liu, J. Tian, L. Wang, H. Li, Y. Zhang and X. Sun, *Macromolecules*, 2010, **43**, 10078–10083.

109 W. Tu, J. Lei, S. Zhang and H. Ju, *Chem.–Eur. J.*, 2010, **16**, 10771–10777.

110 J. Liu, J. Tang and J. J. Gooding, *J. Mater. Chem.*, 2012, **22**, 12435–12452.

111 E. Y. Choi, T. H. Han, J. H. Hong, J. E. Kim, S. H. Lee, H. W. Kim and S. O. Kim, *J. Mater. Chem.*, 2010, **20**, 1907–1912.

112 J. A. Mann and W. R. Dichtel, *J. Phys. Chem. Lett.*, 2013, **4**, 2649–2657.

113 X. An, T. Simmons, R. Shah, C. Wolfe, K. M. Lewis, M. Washington, S. K. Nayak, S. Talapatra and S. Kar, *Nano Lett.*, 2010, **10**, 4295–4301.

114 Y. Liang, D. Wu, X. Feng and K. Müllen, *Adv. Mater.*, 2009, **21**, 1679–1683.

115 J. Geng and H.–T. Jung, *J. Phys. Chem. C*, 2010, **114**, 8227–8234.

116 M. Lotya, P. J. King, U. Khan, S. De and J. N. Coleman, *ACS Nano*, 2010, **4**, 3155–3162.

117 H. Huang, S. Chen, X. Gao, W. Chen and A. T. S. Wee, *ACS Nano*, 2009, **3**, 3431–3436.

118 A. Hirsch, J. M. Englert and F. Hauke, *Acc. Chem. Res.*, 2013, **46**, 87–96.

119 Y. X. Xu, L. Zhao, H. Bai, W. J. Hong, C. Li and G. Q. Shi, *J. Am. Chem. Soc.*, 2009, **131**, 13490–13497.

120 K. Yang, L. Z. Feng, X. Z. Shi and Z. Liu, *Chem. Soc. Rev.*, 2013, **42**, 530–547.

121 K. Yang, S. Zhang, G. Zhang, X. Sun, S.–T. Lee and Z. Liu, *Nano Lett.*, 2010,

10, 3318–3323.

122 E. Wang, M. S. Desai and S.–W. Lee, *Nano Lett.*, 2013, **13**, 2826–2830.

123 L. Baptista–Pires, B. Perez–Lopez, C. C. Mayorga–Martinez, E. Morales–Narvaez, N. Domingo, M. J. Esplandiu, F. Alzina, C. M. Sotomayor–Torres and A. Merkoci, *Biosens. Bioelectron.*, 2014, **61**, 655–662.

124 B. Jiang, K. Yang, Q. Zhao, Q. Wu, Z. Liang, L. Zhang, X. Peng and Y. Zhang, *J. Chromatogr. A*, 2012, **1254**, 8–13.

125 B. Jiang, K. Yang, L. Zhang, Z. Liang, X. Peng and Y. Zhang, *Talanta*, 2014, **122**, 278–284.

126 P. Rani and V. K. Jindal, *RSC Adv.*, 2013, **3**, 802–812.

127 D. Wei, Y. Liu, Y. Wang, H. Zhang, L. Huang and G. Yu, *Nano Lett.*, 2009, **9**, 1752–1758.

128 H. Liu, Y. Liu and D. Zhu, *J. Mater. Chem.*, 2011, **21**, 3335–3345.

129 C. Coletti, C. Riedl, D. S. Lee, B. Krauss, L. Patthey, K. von Klitzing, J. H. Smet and U. Starke, *Phys. Rev. B*, 2010, **81**, 235401.

130 G. Giovannetti, P. Khomyakov, G. Brocks, V. Karpan, J. Van den Brink and P. Kelly, *Phys. Rev. Lett.*, 2008, **101**, 026803.

131 D. Wei and Y. Liu, *Adv. Mater.*, 2010, **22**, 3225–3241.

132 W. Chen, S. Chen, D. C. Qi, X. Y. Gao and A. T. S. Wee, *J. Am. Chem. Soc.*, 2007, **129**, 10418–10422.

133 C. Riedl, C. Coletti and U. Starke, *J. Phys. D: Appl. Phys.*, 2010, **43**, 374009.

134 Z. Chen, I. Santoso, R. Wang, L. F. Xie, H. Y. Mao, H. Huang, Y. Z. Wang, X. Y.

Gao, Z. K. Chen and D. Ma, *Appl. Phys. Lett.*, 2010, **96**, 3104.

135 O. Leenaerts, B. Partoens and F. Peeters, *Phys. Rev. B*, 2008, **77**, 125416.

136 F. Yavari, C. Kritzinger, C. Gaire, L. Song, H. Gulapalli, T. Borca–Tasciuc, P. M. Ajayan and N. Koratkar, *Small*, 2010, **6**, 2535–2538.

137 N. Jung, N. Kim, S. Jockusch, N. J. Turro, P. Kim and L. Brus, *Nano Lett.*, 2009, **9**, 4133–4137.

138 F. Schedin, A. Geim, S. Morozov, E. Hill, P. Blake, M. Katsnelson and K. Novoselov, *Nat. Mater.*, 2007, **6**, 652–655.

139 P. Wei, N. Liu, H. R. Lee, E. Adijanto, L. Ci, B. D. Naab, J. Q. Zhong, J. Park, W. Chen and Y. Cui, *Nano Lett.*, 2013, **13**, 1890–1897.

140 Y. Xue, B. Wu, L. Jiang, Y. Guo, L. Huang, J. Chen, J. Tan, D. Geng, B. Luo and W. Hu, *J. Am. Chem. Soc.*, 2012, **134**, 11060–11063.

141 X. Li, L. Fan, Z. Li, K. Wang, M. Zhong, J. Wei, D. Wu and H. Zhu, *Advanced Energy Materials*, 2012, **2**, 425–429.

142 J. Han, L. L. Zhang, S. Lee, J. Oh, K.–S. Lee, J. R. Potts, J. Ji, X. Zhao, R. S. Ruoff and S. Park, *ACS Nano*, 2012, **7**, 19–26.

143 L. Panchakarla, K. Subrahmanyam, S. Saha, A. Govindaraj, H. Krishnamurthy, U. Waghmare and C. Rao, *Adv. Mater.*, 2009, **21**, 4726–4730.

144 H. Wang, T. Maiyalagan and X. Wang, *ACS Catal.*, 2012, **2**, 781–794.

145 O. S. Kwon, S. J. Park, J.–Y. Hong, A.–R. Han, J. S. Lee, J. S. Lee, J. H. Oh and J. Jang, *ACS Nano*, 2012, **6**, 1486–1493.

146 Z. H. Sheng, L. Shao, J. J. Chen, W.–J. Bao, F. B. Wang and X. H. Xia, *ACS*

Nano, 2011, **5**, 4350–4358.

147 Y. Wang, Y. Shao, D. W. Matson, J. Li and Y. Lin, *ACS Nano*, 2010, **4**, 1790–1798.

148 E. J. Biddinger, D. Von Deak and U. S. Ozkan, *Top. Catal.*, 2009, **52**, 1566–1574.

149 B. Wang, L. Tsetseris, and S. T. Pantelides*, J. Mater. Chem. A,* 2015, **1**, 14927–14934.

150 B. D. Guo, Q. Liu, E. D. Chen, H. W. Zhu, L. Fang, and J. R. Gong, *Nano Lett*., 2010, **10**, 4975–4980.

151 P. Wu, P. Du, H. Zhang and C. Cai, *Phys. Chem. Chem. Phys.*, 2013, **15**, 6920–6928.

152 X. Wang, G. Sun, P. Routh, D.–H. Kim, W. Huang and P. Chen, *Chem. Soc. Rev.*, 2014, **43**, 7067–7098.

153 S. Jalili and R. Vaziri, *Mol. Phys.*, 2011, **109**, 687–694.

154 T. Schiros, D. Nordlund, L. Pálová, D. Prezzi, L. Zhao, K. S. Kim, U. Wurstbauer, C. Gutiérrez, D. Delongchamp and C. Jaye, *Nano Lett.*, 2012, **12**, 4025–4031.

155 T. Schiros, D. Nordlund, L. Palova, D. Prezzi, L. Y. Zhao, K. S. Kim, U. Wurstbauer, C. Gutierrez, D. Delongchamp, C. Jaye, D. Fischer, H. Ogasawara, L. G. M. Pettersson, D. R. Reichman, P. Kim, M. S. Hybertsen and A. N. Pasupathy, *Nano Lett.*, 2012, **12**, 4025–4031.

156 Y. Liu, Q. Feng, N. Tang, X. Wan, F. Liu, L. Lv and Y. Du, *Carbon*, 2013, **60**,

549–551.

157 Y. Li, Z. Zhou, P. Shen and Z. Chen, *ACS Nano*, 2009, **3**, 1952–1958.

158 J. Chiou, S. C. Ray, S. Peng, C. Chuang, B. Wang, H. Tsai, C. Pao, H.–J. Lin, Y. Shao and Y. Wang, *J. Phys. Chem. C*, 2012, **116**, 16251–16258.

159 Z. Jin, J. Yao, C. Kittrell and J. M. Tour, *ACS Nano*, 2011, **5**, 4112–4117.

160 J. Ortiz‐Medina, M. L. García‐Betancourt, X. Jia, R. Martínez‐Gordillo, M. A. Pelagio‐Flores, D. Swanson, A. L. Elías, H. R. Gutiérrez, E. Gracia‐Espino and V. Meunier, *Adv. Funct. Mater.*, 2013, **23**, 3755–3762.

161 X. Li, H. Wang, J. T. Robinson, H. Sanchez, G. Diankov and H. Dai, *J. Am. Chem. Soc.*, 2009, **131**, 15939–15944.

162 Z.–S. Wu, S. Yang, Y. Sun, K. Parvez, X. Feng and K. Müllen, *J. Am. Chem. Soc.*, 2012, **134**, 9082–9085.

163 P. Rani and V. Jindal, *RSC Adv.*, 2013, **3**, 802–812.

164 R. Faccio, L. Fernández–Werner, H. Pardo, C. Goyenola, O. N. Ventura and Á. W. Mombrú, *J. Phys. Chem. C*, 2010, **114**, 18961–18971.

165 Z. H. Sheng, H. L. Gao, W. J. Bao, F. B. Wang and X. H. Xia, *J. Mater. Chem.*, 2012, **22**, 390–395.

166 Y. B. Tang, L. C. Yin, Y. Yang, X. H. Bo, Y. L. Cao, H. E. Wang, W. J. Zhang, I. Bello, S. T. Lee and H. M. Cheng, *ACS Nano*, 2012, **6**, 1970–1978.

167 S. Kawai, S. Saito, S. Osumi. S. Yamaguchi, A. S. Foster, P. Spijker, and E. Meyer, Nat. Commun., 2015, 6, 8089. DOI: 10.1038/ncomms8098 (2015).

168 O. L. Stroyuk, N. S. Andryushina, S. Y. Kuchmy and V. D. Pokhodenko, *Theor.*

Exp. Chem., 2015, **51**, 1–29.

169 L. Zhou, L. Zhang, L. Liao, M. Yang, Q. Xie, H. Peng, Z. Liu and Z. Liu, *Acta Chim. Sinica*, 2014, **72**, 289–300.

170 L. Zhang, L. Zhou, M. Yang, Z. Liu, Q. Xie and H. Peng, *Small*, 2013, **9**, 1134–1143.

171 S. C. Zhao, S. P. Surwade, Z. T. Li and H. T. Liu, *Nanotechnology*, 2012, **23**, 355703.

172 W.–C. Hou, I. Chowdhury, D. G. Goodwin Jr, W. M. Henderson, D. H. Fairbrother, D. Bouchard and R. G. Zepp, *Environ. Sci. Technol.*, 2015, **49**, 3435–3443.

173 O. Fellahi, M. R. Das, Y. Coffinier, S. Szunerits, T. Hadjersi, M. Maamache and R. Boukherroub, *Nanoscale*, 2011, **3**, 4662–4669.

174 P. Kumar, K. Subrahmanyam and C. Rao, *International Journal of Nanoscience*, 2011, **10**, 559–566.

175 H. T. Liu, S. M. Ryu, Z. Y. Chen, M. L. Steigerwald, C. Nuckolls and L. E. Brus, *J. Am. Chem. Soc.*, 2009, **131**, 17099–17101.

176 L. Zhang, L. Zhou, M. Yang, Z. Liu, Q. Xie, H. Peng and Z. Liu, *Small*, 2013, **9**, 1134–1143.

177 H. Li, S. Pang, X. Feng, K. Mullen and C. Bubeck, *Chem. Commun.*, 2010, **46**, 6243–6245.

178 Y. Matsumoto, M. Koinuma, S. Y. Kim, Y. Watanabe, T. Taniguchi, K. Hatakeyama, H. Tateishi and S. Ida, *ACS Appl. Mater. Inter.*, 2010, **2**, 3461–

3466.

179 W. H. Lee, J. W. Suk, H. Chou, J. H. Lee, Y. F. Hao, Y. P. Wu, R. Piner, D. Aldnwande, K. S. Kim and R. S. Ruoff, *Nano Lett.*, 2012, **12**, 2374–2378.

180 L.–H. Liu, G. Zorn, D. G. Castner, R. Solanki, M. M. Lerner and M. Yan, *J. Mater. Chem.*, 2010, **20**, 5041–5046.

181 B. Li, L. Zhou, D. Wu, H. L. Peng, K. Yan, Y. Zhou and Z. F. Liu, *ACS Nano*, 2011, **5**, 5957–5961.

182 M. M. Yang, L. Zhou, J. Y. Wang, Z. F. Liu and Z. R. Liu, *J. Phys. Chem. C*, 2012, **116**, 844–850.

183 R. R. Nair, W. C. Ren, R. Jalil, I. Riaz, V. G. Kravets, L. Britnell, P. Blake, F. Schedin, A. S. Mayorov, S. J. Yuan, M. I. Katsnelson, H. M. Cheng, W. Strupinski, L. G. Bulusheva, A. V. Okotrub, I. V. Grigorieva, A. N. Grigorenko, K. S. Novoselov and A. K. Geim, *Small*, 2010, **6**, 2877–2884.

184 S. B. Bon, L. Valentini, R. Verdejo, J. L. G. Fierro, L. Peponi, M. A. Lopez–Manchado and J. M. Kenny, *Chem. Mater.*, 2009, **21**, 3433–3438.

185 Y. Matsumoto, M. Morita, S. Y. Kim, Y. Watanabe, M. Koinuma and S. Ida, *Chem. Lett.*, 2010, **39**, 750–752.

186 R. Y. Gengler, D. S. Badali, D. Zhang, K. Dimos, K. Spyrou, D. Gournis and R. D. Miller, *Nat. Commun.*, 2013, **4**, 2560.

187 Y. L. Zhang, L. Guo, H. Xia, Q. D. Chen, J. Feng and H. B. Sun, *Adv. Opt. Mater.*, 2014, **2**, 10–28.

188 X.–H. Li, J.–S. Chen, X. Wang, M. E. Schuster, R. Schloegl and M. Antonietti,

Chemsuschem, 2012, **5**, 642–646.

189 L. Huang, Y. Liu, L. C. Ji, Y. Q. Xie, T. Wang and W. Z. Shi, *Carbon*, 2011, **49**, 2431–2436.

190 M. F. El–Kady, V. Strong, S. Dubin and R. B. Kaner, *Science*, 2012, **335**, 1326–1330.

191 C. Petridis, Y.–H. Lin, K. Savva, G. Eda, E. Kymakis, T. Anthopoulos and E. Stratakis, *Appl. Phys. Lett.*, 2013, **102**, 093115.

192 V. Strong, S. Dubin, M. F. El–Kady, A. Lech, Y. Wang, B. H. Weiller and R. B. Kaner, *ACS Nano*, 2012, **6**, 1395–1403.

193 X. Fan, G. Zhang and F. Zhang, *Chem. Soc. Rev.*, 2015, **44**, 3023–3035.

194 B. Y. Xia, Y. Yan, X. Wang and X. W. Lou, *Materials Horizons*, 2014, **1**, 379–399.

195 X. Wang, C. Li and G. Shi, *Phys. Chem. Chem. Phys.*, 2014, **16**, 10142–10148.

196 D. R. Dreyer, H.–P. Jia and C. W. Bielawski, *Angew. Chem. Int. Ed.*, 2010, **49**, 6813–6816.

197 D. W. Boukhvalov, D. R. Dreyer, C. W. Bielawski and Y.–W. Son, *ChemCatChem*, 2012, **4**, 1844–1849.

198 S. Tang and Z. Cao, *Phys. Chem. Chem. Phys.*, 2012, **14**, 16558–16565.

199 Y. Song, K. Qu, C. Zhao, J. Ren and X. Qu, *Adv. Mater.*, 2010, **22**, 2206–2210.

200 Y. Gao, D. Ma, C. Wang, J. Guan and X. Bao, *Chem. Commun.*, 2011, **47**, 2432–2434.

201 W. Zhang, S. Wang, J. Ji, Y. Li, G. Zhang, F. Zhang and X. Fan, *Nanoscale*,

2013, **5**, 6030–6033.

202 L. Tan, B. Wang and H. Feng, *RSC Adv.*, 2013, **3**, 2561–2565.

203 S. Y. Oh, J. G. Son, S. H. Hur, J. S. Chung and P. C. Chiu, *J. Environ. Qual.*, 2013, **42**, 815–821.

204 L. Feng, Y. Chen and L. Chen, *ACS Nano*, 2011, **5**, 9611–9618.

205 H. Kim, K. Lee, S. I. Woo and Y. Jung, *Phys. Chem. Chem. Phys.*, 2011, **13**, 17505–17510.

206 L. Lai, J. R. Potts, D. Zhan, L. Wang, C. K. Poh, C. Tang, H. Gong, Z. Shen, J. Lin and R. S. Ruoff, *Energy Environ. Sci.*, 2012, **5**, 7936–7942.

207 L. P. Zhang and Z. H. Xia, *J. Phys. Chem. C*, 2011, **115**, 11170–11176.

208 S. Yang, X. Feng, X. Wang and K. Müllen, *Angew. Chem. Int. Ed.*, 2011, **50**, 5339–5343.

209 P. Wang, Z. Wang, L. Jia and Z. Xiao, *Phys. Chem. Chem. Phys.*, 2009, **11**, 2730–2740.

210 Z. S. Wu, A. Winter, L. Chen, Y. Sun, A. Turchanin, X. Feng andK. Müllen, *Adv. Mater.*, 2012, **24**, 5130–5135.

211 J. Liang, Y. Jiao, M. Jaroniec and S. Z. Qiao, *Angew. Chem. Int. Ed.*, 2012, **51**, 11496–11500.

212 F. Liu, J. Sun, L. Zhu, X. Meng, C. Qi and F. S. Xiao, *J. Mater. Chem.*, 2012, **22**, 5495–5502.

213 X. Sun, W. Wang, T. Wu, H. Qiu, X. Wang and J. Gao, *Mater. Chem. Phys.*, 2013, **138**, 434–439.

214 N. Behabtu, J. R. Lomeda, M. J. Green, A. L. Higginbotham, A. Sinitskii, D. V. Kosynkin, D. Tsentalovich, A. N. G. Parra–Vasquez, J. Schmidt and E. Kesselman, *Nat. Nanotechnol.*, 2010, **5**, 406–411.

215 Z. Xu and C. Gao, *ACS Nano*, 2011, **5**, 2908–2915.

216 Z. Xu and C. Gao, *Nat. Commun.*, 2011, **2**, 9.

217 Z. Xu and C. Gao, *Acc. Chem. Res.*, 2014, **47**, 1267–1276.

218 Z. Xu, H. Sun, X. Zhao and C. Gao, *Adv. Mater.*, 2013, **25**, 188–193.

219 Z. Hongju, C. Chong, Q. Hui, M. Lang, H. Chao, N. Shengqiang, Z. Xiang, F. Qiang and Z. Changsheng, *Polym. Chem.*, 2014, **5**, 3563–3575.

220 J.–J. Shao, W. Lv and Q.–H. Yang, *Adv. Mater.*, 2014, **26**, 5586–5612.

221 D. A. Dikin, S. Stankovich, E. J. Zimney, R. D. Piner, G. H. B. Dommett, G. Evmenenko, S. T. Nguyen and R. S. Ruoff, *Nature*, 2007, **448**, 457–460.

222 S. Park, N. Mohanty, J. W. Suk, A. Nagaraja, J. An, R. D. Piner, W. Cai, D. R. Dreyer, V. Berry and R. S. Ruoff, *Adv. Mater.*, 2010, **22**, 1736–1740.

223 H. Chen, M. B. Müller, K. J. Gilmore, G. G. Wallace and D. Li, *Adv. Mater*, 2008, **20**, 3557–3561.

224 C. Vallés, J. D. Núñez, A. M. Benito and W. K. Maser, *Carbon*, 2012, **50**, 835–844.

225 H. Bai, C. Li, X. L. Wang and G. Q. Shi, *Chem. Commun.*, 2010, **46**, 2376–2378.

226 Y. X. Xu, K. X. Sheng, C. Li and G. Q. Shi, *ACS Nano*, 2010, **4**, 4324–4330.

227 H. Bai, K. X. Sheng, P. F. Zhang, C. Li and G. Q. Shi, *J. Mater. Chem.*, 2011, **21**,

18653–18658.

228 Z. Tang, S. Shen, J. Zhuang and X. Wang, *Angew. Chem.*, 2010, **122**, 4707–4711.

229 C. Huang, H. Bai, C. Li and G. Shi, *Chem. Commun.*, 2011, **47**, 4962–4964.

230 X. Jiang, Y. Ma, J. Li, Q. Fan and W. Huang, *J. Phys. Chem. C*, 2010, **114**, 22462–22465.

231 S. Sun and P. Wu, *J. Mater. Chem.*, 2011, **21**, 4095–4097.

232 H. Bai, C. Li, X. L. Wang and G. Q. Shi, *J. Phys. Chem. C*, 2011, **115**, 5545–5551.

233 W. Chen, S. Li, C. Chen and L. Yan, *Adv. Mater.*, 2011, **23**, 5679–5683.

234 C. Li and G. Q. Shi, *Adv. Mater.*, 2014, **26**, 3992–4012.

235 Y. R. Li, J. Chen, L. Huang, Dr C. Li, J. D. Hong and G. Q. Shi, *Adv. Mater.*, 2014, **26**, 4789–4793

236 H.–P. Cong, X.–C. Ren, P. Wang and S.–H. Yu, *ACS Nano*, 2012, **6**, 2693–2703.

237 S. Chen, J. Duan, Y. Tang and S. Zhang Qiao, *Chem.–Eur. J.*, 2013, **19**, 7118–7124.

238 Y. Zhao, J. Liu, Y. Hu, H. Cheng, C. Hu, C. Jiang, L. Jiang, A. Cao and L. Qu, *Adv. Mater.*, 2013, **25**, 591–595.

239 K. X. Sheng, Y. X. Xu, C. Li and G. Q. Shi, *New Carbon Mater.*, 2011, **26**, 1–6.

240 J. Chen, K. X. Sheng, P. H. Luo, C. Li and G. Q. Shi, *Adv. Mater.*, 2012, **24**, 4569–4573.

241 K. X. Sheng, Y. Q. Sun, C. Li, W. J. Yuan and G. Q. Shi, *Sci. Rep*., 2012, **2**, 247.

242 X. W. Yu, K. X. Sheng and G. Q. Shi, *Analyst*, 2014, **139**, 4525–4531.

243 X. W. Yu, M. Zhang, W. J. Yuan and G. Q. Shi, *J. Mater. Chem. A*, 2015, **3**, 6921–6928.

Xiluan Wang received her B. Eng. degree (2010) and Ph. D. degree (2015) from Beijing University of Chemical Technology and Tsinghua University. She is currently working in Beijing Forestry University as a lecturer. Her research interests focus on the synthesis and applications of chemically modified graphene.

Prof. Gaoquan Shi received his BS degree (1985) and PhD degree (1992) at the Department of Chemistry, Nanjing University. Then he joined Nanjing University and was promoted to full professor in 1995. In 2000, he moved to Tsinghua University as a Professor of Chemistry. His research interests are focused on synthesis and applications of graphene materials and conducting polymers. He received the 2nd Grade Award of Natural Science of China and the Youth Knowledge Innovation Prize of the Chinese Chemical Society and BASF Company in 2004, and the 1st Grade Award of Natural Science of Chinese Education Ministry in 2013.